5. Rupprecht HD, Dann P, Sukhatme VP, *et al*: Effect of vasoactive agents on induction of Egr-1 in rat mesangial cells: correlation with mitogenicity. *Am J Physiol* 263:F623–F636, 1992
6. Sukhatme VP, Kartha S, Toback FG, *et al*: A novel early growth response gene rapidly induced by fibroblast, epithelial cell and lymphocyte mitogens. *Oncogene Res* 1:343–355, 1987
7. Sukhatme VP, Cao XM, Chang LC, *et al*: A zinc finger-encoding gene coregulated with c-fos during growth and differentiation, and after cellular depolarization. *Cell* 53:37–43, 1988
8. Nguyen HQ, Hoffman-Liebermann B, Liebermann DA: The zinc finger transcription factor Egr-1 is essential for and restricts differentiation along the macrophage lineage. *Cell* 72:197–209, 1993
9. Hallahan DE, Sukhatme VP, Sherman ML, *et al*: Protein kinase C mediates x-ray inducibility of nuclear signal transducers EGR1 and JUN. *Proc Natl Acad Sci USA* 88:2156–2160, 1991
10. Yan SF, Lu J, Zou YS, *et al*: Hypoxia-associated induction of early growth response-1 gene expression. *J Biol Chem* 274:15030–15040, 1999
11. Yan SF, Zou YS, Gao Y, *et al*: Tissue factor transcription driven by Egr-1 is a critical mechanism of murine pulmonary fibrin deposition in hypoxia. *Proc Natl Acad Sci USA* 95:8298–8303, 1998
12. Nair P, Muthukkumar S, Sells SF, *et al*: Early growth response-1-dependent apoptosis is mediated by p53. *J Biol Chem* 272:20131–20138, 1997
13. Gashler A, Sukhatme VP: Early growth response protein 1 (Egr-1): Prototype of a zinc-finger family of transcription factors. *Prog Nucleic Acid Res Mol Biol* 50:191–224, 1995
14. Rupprecht HD, Sukhatme VP, Rupprecht AP, *et al*: Serum response elements mediate protein kinase C dependent transcriptional induction of early growth response gene-1 by arginine vasopressin in rat mesangial cells. *J Cell Physiol* 159:311–323, 1994
15. Rupprecht HD, Sukhatme VP, Lacy J, *et al*: PDGF-induced Egr-1 expression in rat mesangial cells is mediated through upstream serum response elements. *Am J Physiol* 265:F351–F360, 1993
16. Arsenian S, Weinhold B, Oelgeschlager M, *et al*: Serum response factor is essential for mesoderm formation during mouse embryogenesis. *EMBO J* 17:6289–6299, 1998
17. Khachigian LM, Williams AJ, Collins T: Interplay of Sp1 and Egr-1 in the proximal platelet-derived growth factor A-chain promoter in cultured vascular endothelial cells. *J Biol Chem* 270: 27679–27686, 1995
18. Silverman ES, Khachigian LM, Lindner V, *et al*: Inducible PDGF A-chain transcription in smooth muscle cells is mediated by Egr-1 displacement of Sp1 and Sp3. *Am J Physiol* 273:H1415–H1426, 1997
19. Khachigian LM, Collins T: Inducible expression of Egr-1-dependent genes. A paradigm of transcriptional activation in vascular endothelium. *Circ Res* 81:457–461, 1997
20. Biesiada E, Razandi M, Levin ER: Egr-1 activates basic fibroblast growth factor transcription. Mechanistic implications for astrocyte proliferation. *J Biol Chem* 271:18576–18581, 1996
21. Kim SJ, Jeang KT, Glick AB, *et al*: Promoter sequences of the human transforming growth factor-beta 1 gene responsive to transforming growth factor-beta 1 autoinduction. *J Biol Chem* 264:7041–7045, 1989
22. Shingu T, Bornstein P: Overlapping Egr-1 and Sp1 sites function in the regulation of transcription of the mouse thrombospondin 1 gene. *J Biol Chem* 269:32551–32557, 1994
23. Maltzman JS, Carman JA, Monroe JG: Role of EGR1 in regulation of stimulus-dependent CD44 transcription in B lymphocytes. *Mol Cell Biol* 16:2283–2294, 1996
24. Maltzman JS, Carmen JA, Monroe JG: Transcriptional regulation of the Icam-1 gene in antigen receptor- and phorbol ester-stimulated B lymphocytes: Role for transcription factor EGR1. *J Exp Med* 183:1747–1759, 1996
25. Yan YX, Nakagawa H, Lee MH, Rustgi AK: Transforming growth factor-alpha enhances cyclin D1 transcription through the binding of early growth response protein to a cis-regulatory element in the cyclin D1 promoter. *J Biol Chem* 272:33181–33190, 1997
26. Kinane TB, Finder JD, Kawashima A, *et al*: Growth of LLC-PK1 renal cells is mediated by EGR-1 up-regulation of G protein alpha i-2 protooncogene transcription. *J Biol Chem* 269:27503–27509, 1994
27. Lee SL, Tourtellotte LC, Wesselschmidt RL, Milbrandt J: Growth and differentiation proceeds normally in cells deficient in the immediate early gene NGFI-A. *J Biol Chem* 270:9971–9977, 1995
28. Lee SL, Sadovsky Y, Swirnoff AH, *et al*: Luteinizing hormone deficiency and female infertility in mice lacking the transcription factor NGFI-A (Egr-1). *Science* 273:1219–1221, 1996
29. Cui MZ, Parry GC, Oeth P, *et al*: Transcriptional regulation of the tissue factor gene in human epithelial cells is mediated by Sp1 and EGR-1. *J Biol Chem* 271:2731–2739, 1996
30. Day ML, Zhao X, Wu S, *et al*: Phorbol ester-induced apoptosis is accompanied by NGFI-A and c-fos activation in androgen-sensitive prostate cancer cells. *Cell Growth Differ* 5:735–741, 1994
31. Eid MA, Kumar MV, Iczkowski KA, *et al*: Expression of early growth response genes in human prostate cancer. *Cancer Res* 58:2461–2468, 1998
32. Thigpen AE, Cala KM, Guileyardo JM, *et al*: Increased expression of early growth response-1 messenger ribonucleic acid in prostatic adenocarcinoma. *J Urol* 155:975–981, 1996
33. Abdulkadir SA, Qu Z, Garabedian E, *et al*: Impaired prostate tumorigenesis in *Egr1*-deficient mice. *Nat Med* 7:101–107, 2001
34. Khachigian LM, Lindner V, Williams AJ, Collins T: *Egr-1*-induced endothelial gene expression: a common theme in vascular injury. *Science* 271:1427–1431, 1996
35. Gousseva N, Kugathasan K, Chesterman CN, Khachigian LM: Early growth response factor-1 mediates insulin-inducible vascular endothelial cell proliferation and regrowth after injury. *J Cell Biochem* 81:523–534, 2001
36. Santiago FS, Atkins DG, Khachigian LM: Vascular smooth muscle cell proliferation and regrowth after mechanical injury in vitro are *Egr-1*/NGFI-A-dependent. *Am J Pathol* 155:897–905, 1999
37. Santiago FS, Lowe HC, Day FL, *et al*: Early growth response factor-1 induction by injury is triggered by release and paracrine activation by fibroblast growth factor-2. *Am J Pathol* 154:937–944, 1999
38. Santiago FS, Lowe HC, Kavurma MM, *et al*: New DNA enzyme targeting *Egr-1* mRNA inhibits vascular smooth muscle proliferation and regrowth after injury. *Nat Med* 5:1264–1269, 1999
39. McCaffrey TA, Fu C, Du B, *et al*: High-level expression of *Egr-1* and *Egr-1*-inducible genes in mouse and human atherosclerosis. *J Clin Invest* 105:653–662, 2000
40. Rupprecht HD, Akagi Y, Keil A, Hofer G: Nitric oxide inhibits growth of glomerular mesangial cells: Role of the transcription factor EGR-1. *Kidney Int* 57:70–82, 2000
41. Imai E, Isaka Y, Akagi Y, Kaneda Y: Gene transfer into the glomerulus by the hemagglutinating virus of Japan-liposome method. *Exp Nephrol* 5:112–117, 1997
42. Akagi Y, Isaka Y, Arai M, *et al*: Inhibition of TGF-beta 1 expression by antisense oligonucleotides suppressed extracellular matrix accumulation in experimental glomerulonephritis. *Kidney Int* 50: 148–155, 1996
43. Arai M, Wada A, Isaka Y, *et al*: In vivo transfection of genes for renin and angiotensinogen into the glomerular cells induced phenotypic change of the mesangial cells and glomerular sclerosis. *Biochem Biophys Res Commun* 206:525–532, 1995
44. Tomita N, Higaki J, Morishita R, *et al*: Direct in vivo gene introduction into rat kidney. *Biochem Biophys Res Commun* 186:129–134, 1992
45. Bagchus WM, Hoedemaeker PJ, Rozing J, Bakker WW: Glomerulonephritis induced by monoclonal anti-Thy 1.1 antibodies. A sequential histological and ultrastructural study in the rat. *Lab Invest* 55:680–687, 1996
46. Isaka Y, Akagi Y, Kaneda Y, Imai E: The HVJ liposome method. *Exp Nephrol* 6:144–147, 1998
47. Isaka Y, Fujiwara Y, Ueda N, *et al*: Glomerulosclerosis induced by in vivo transfection of transforming growth factor-beta or platelet-derived growth factor gene into the rat kidney. *J Clin Invest* 92:2597–2601, 1993
48. Johnson RJ, Raines EW, Floege J, *et al*: Inhibition of mesangial cell proliferation and matrix expansion in glomerulonephritis in the rat by antibody to platelet-derived growth factor. *J Exp Med* 175:1413–1416, 1992
49. Floege J, Ostendorf T, Janssen U, *et al*: Novel approach to specific growth factor inhibition in vivo: Antagonism of platelet-derived growth factor in glomerulonephritis by aptamers. *Am J Pathol* 154:169–179, 1999

Kidney International, Vol. 63 (2003), pp. 1861–1867

The efficacy of tonsillectomy on long-term renal survival in patients with IgA nephropathy

YUANSHENG XIE, SHINICHI NISHI, MITSUHIRO UENO, NAOFUMI IMAI, MINORU SAKATSUME, ICHIEI NARITA, YASUSHI SUZUKI, KOUHEI AKAZAWA, HISAKI SHIMADA, MASAAKI ARAKAWA, and FUMITAKE GEJYO

Division of Clinical Nephrology and Rheumatology, Niigata University Graduate School of Medical and Dental Sciences, Niigata, Japan; Saiseikai Niigata Daini Hospital, Niigata, Japan; Department of Medical Informatics, Niigata University Medical Hospital, Niigata, Japan; Internal Medicine, Niigata Prefectural Central Hospital, Jyoetsu, Japan; and Department of Health & Social Welfare and Bureau of Hospital Administration, Niigata Prefectural Government, Niigata, Japan

The efficacy of tonsillectomy on long-term renal survival in patients with IgA nephropathy.

Background. Little information has been available until now about the clinical efficacy of tonsillectomy on long-term renal survival of patients with idiopathic immunoglobulin A nephropathy (IgAN).

Methods. To investigate the effect of tonsillectomy on long-term renal survival, we reviewed the clinical course of 118 patients with idiopathic biopsy-diagnosed IgAN from 1973 to 1980. Of those, 48 patients received tonsillectomy and 70 patients did not. The starting point of observation was defined as the time of the diagnostic renal biopsy, and the end point as when requiring the first dialysis. Up to 2001, the mean observation time was 192.9 ± 74.8 months (48–326 months). Renal survival and impact of covariates were evaluated by Kaplan-Meier analysis and Cox proportional hazards regression model.

Results. Age, gender, amount of urinary protein excretion, serum creatinine, serum IgA, blood pressure, and histopathologic findings at the time of renal biopsy and treatments during the observation period were not significantly different between patients with and without tonsillectomy. Five (10.4%) of the patients with tonsillectomy and 18 (25.7%) of the patients without tonsillectomy finally required dialysis therapy (chi-square test, $P = 0.0393$). By Kaplan-Meier analysis, renal survival rates were 89.6% and 63.7% at 240 months in the patients with and without tonsillectomy, respectively, and were significantly different (log-rank test, $P = 0.0329$). In the multivariate Cox regression model, tonsillectomy (hazard ratio, 0.22; 95% CI, 0.06 to 0.76; $P = 0.0164$) had a significant effect on renal outcome.

Conclusion. These results indicate that tonsillectomy has a favorable effect on long-term renal survival in patients with IgAN.

Key words: tonsillectomy, immunoglobulin A nephropathy, renal survival.

Received for publication August 12, 2002
and in revised form November 1, 2002
Accepted for publication January 3, 2003

Immunoglobulin A nephropathy (IgAN), which is characterized by glomerular mesangial proliferation with a predominant IgA deposition in the mesangial areas, is the most common glomerulonephritis worldwide, accounting for 25% to 50% among primary glomerulonephritis [1–3]. IgAN was initially considered a benign disease, but long-term follow-up studies have shown the course to be progressive with up to 50% of patients developing terminal renal failure after several decades [3–6]. Even IgAN with hematuria and minimal proteinuria is usually progressive and life-long follow-up with regular monitoring is recommended [7]. Since the pathogenesis of IgAN is obscure, specific treatment is not yet available. Previous approaches have included tonsillectomy, prednisolone, immunosuppressants, antihypertension drugs, anticoagulants, fish oils, and others [8–10].

Although tonsillectomy has been expected to show efficacy, up to now there has been little information about the clinical effect of tonsillectomy on long-term renal survival in which the mean observation time exceeded 10 years in patients with IgAN. Previous studies demonstrated that half of the patients with IgAN showed distinct improvement in urinary findings or/and the levels of serum IgA, the circulating immune complex and serum polymeric IgA, several months or several years after tonsillectomy [11–13]. Recently, Hotta et al [14] used Cox proportional hazards model and reported that a combination of tonsillectomy and steroid pulse therapy had a significant impact on clinical remission, defined as negative proteinuria and hematuria, in IgAN patients with a median follow-up duration of 75 months, but the impact of tonsillectomy on long-term renal survival was unclear. In addition, the clinical benefit of tonsillectomy in patients with IgAN remains controversial. Rasche, Schwarz, and Keller [15] estimated the probability of renal survival 10 years after renal biopsy and the impact

of risk factors in patients with IgAN by Kaplan-Meier analysis and Cox regression model. The results were not significantly different between 16 patients with tonsillectomy and 39 patients without tonsillectomy. Their mean observation time after renal biopsy was relatively short (3.4 ± 4 years) in that study.

To clearly establish the effect of tonsillectomy on long-term renal survival, we compared the clinical course of IgAN patients with and without tonsillectomy in which the mean observation time was over 15 years, and estimated renal survival and the impact of multiple covariates, including clinical and pathologic findings, on the prognosis by Kaplan-Meier analysis and Cox regression model. The results showed that tonsillectomy had a favorable effect on long-term renal survival in patients with IgAN.

METHODS

Patients

Among 555 patients who underwent renal biopsy and immunofluorenscence examination between 1973 and 1980, we identified 162 inpatients with IgAN followed-up at our department. The diagnosis was limited to primary glomerulonephritis with a predominant deposition of IgA in the mesangium. No patients had clinical or histologic evidence of systemic diseases as systemic lupus erythematosus, Henoch-Schönlein purpura, or chronic liver disease. Exclusion criteria for the present study were a follow-up period less than 48 months. As a result, 118 of the 162 patients with IgAN were included in this study. Forty-eight patients underwent tonsillectomy, and 70 patients did not, before or after renal biopsy.

Follow-up and outcome measures

At the time of the annual birthday of every patient after renal biopsy, letters were sent to each one inviting them to our hospital or affiliated hospitals for examinations of blood pressure, urinalysis, and renal function. Then, we stored the results of the examinations or current physical status and treatment (living or dead, requiring dialysis or not, and any treatment or not) in a computer data bank.

The starting point of observation in this study was defined as the time of the diagnostic renal biopsy, and the end point as the time when the first dialysis was required. All patients in this study were followed up for more than 48 months. Renal survival was defined as dialysis-free.

Clinical, laboratory, and pathologic data

Baseline clinical and laboratory data at the time of the diagnostic renal biopsy were chosen from primary case records. Patient characteristics included age, gender, and mean arterial pressure calculated from systolic pressure and diastolic pressure, degree of proteinuria and hematuria, serum creatinine and serum IgA level. If the amount of urine protein excretion was less than 0.1 g/24 hours, it was considered to be 0.1 g/24 hours. The numbers of urine red blood cells with macrohematuria were defined as 100/high power field when calculating. The histologic score was from primary pathologic diagnostic reports using light microcopy. The severity of glomerular mesangial proliferation, global glomerular sclerosis, interstitial lesions, and crescent formation in each case was graded semiquantitatively from 0 to 4, according to the percentage of injured tissue, respectively. The grades were as follows: 0 = no lesion (or interstitial lesions were less than 5%); 1 = <25% (interstitial lesion was defined as ≥5% and <25%); 2 = ≥25% and <50%; 3 = ≥50% and <75%; and 4 = ≥75%.

Tonsillectomy and drug therapy

Almost all IgAN patients had their tonsils checked and underwent bacterial culture by otolaryngologists during hospitalization in a clinical nephrology division, even those without tonsillectomy. The indication for tonsillectomy in patients with IgAN was chronic tonsillitis or a positive tonsil provocation test estimated by otolaryngologists. Chronic tonsillitis included chronic hypertrophic tonsillitis and chronic atrophic tonsillitis. The latter was the prevalent form in adult chronic tonsillitis and mainly revealed cryptic large tonsils with inflammatory debris or fibrotic tonsils because of recurrent infection and scarring. Adoption of tonsillectomy arbitrarily depended on the will of each patient or the recommendation of physicians after examination by otolaryngologists. Tonsillectomy was performed before, during, or after hospitalization for a diagnostic renal biopsy.

Drug therapies included steroid (prednisolone), immunosuppressant (cyclophosphamide or azathioprine), antiplatelet or anticoagulant (dipyridamole or warfarin), and antihypertension [diuretics, β blockers, α blockers, calcium antagonists, angiotensin-converting enzyme (ACE) inhibitors and others] therapies during follow-up. Data regarding the treatments were recorded from primary medical records and the outcomes of follow-up, such as outclinic records and questionnaires. Most patients were not given any drugs during follow-up according to the policy two decades ago.

Statistical analysis

We used the chi-square test to analyze the frequency of categorical variables. Differences in the continuous variables between the groups were compared using the Mann-Whitney U test (Wilcoxon rank sum test) and the unpaired *t* test (Student *t* test). As the results were similar, only the latter are presented. The renal survival curves and cumulative renal survival rates for IgAN patients in the groups were calculated using the Kaplan-

Table 1. Baseline characteristics of the patients with immunoglobulin A nephropathy (IgAN)

Characteristic	Tonsillectomy $N = 48$	Non-tonsillectomy $N = 70$	P value
At the time of biopsy			
Male/female	28/20	36/34	NS
Age *years*	30.35 ± 11.46	33.64 ± 12.03	NS
Mean arterial pressure *mm Hg*	97.39 ± 12.66	96.71 ± 12.64	NS
Urine red blood cells */high power field*	39.53 ± 43.00	44.58 ± 42.77	NS
Urine protein *g/24 hours*	0.91 ± 1.12	1.09 ± 1.43	NS
Serum creatinine *mg/dL*	1.07 ± 0.27	1.07 ± 0.31	NS
Serum IgA *mg/dL*	375.7 ± 131.0	363.9 ± 125.4	NS
Chronic tonsillitis +	31	41	NS
Pathologic finding			
Mesangial proliferation	2.73 ± 0.73	2.47 ± 0.92	NS
Global glomerular sclerosis	0.77 ± 0.94	0.90 ± 1.00	NS
Interstitial lesion	0.77 ± 0.77	0.89 ± 0.96	NS
Crescent formation	0.46 ± 0.66	0.34 ± 0.60	NS
Background therapy			
Antihypertension	14	14	NS
Steroid	4	13	NS
Immunosuppressant	4	13	NS
Antiplatelet	5	15	NS
No drugs	27	32	NS

NS is not significant. Data = mean ± SD. The damage severity of renal biopsy tissue was graded from 0 to 4 according to the percentage of the lesion range, respectively. 0 = No lesion (or interstitial lesions were <5%); 1 = <25% (interstitial lesion was defined as ≥5% and <25%); 2 = ≥25% and <50%; 3 = ≥50% and <75%; and 4 = ≥75%. Antihypertension drugs included diuretics, β blockers, α blockers, calcium antagonists, angiotensin-converting enzyme inhibitors and others. Steroids included prednisolone. Immunosuppressants included cyclophosphamide or azathioprine. Antiplatelets included dipyridamole or warfarin.

Meier analysis. Comparisons of the time course from renal biopsy to end points between the groups were performed by means of a log-rank test. To estimate the size of the effect, we used a Cox regression model, choosing a forward stepwise procedure to assess the impact of multiple covariates for renal prognosis. Variables used in multivariable analysis were expressed using a binary scale, such as absent/present, and coded as 0/1. Mean arterial pressure, amount of urine protein excretion, serum creatinine level, global glomerular sclerosis, interstitial lesions, crescent formation, steroid therapy, and tonsillectomy were treated as categoric variables. The results of multivariable analysis were expressed by a hazard ratio and 95% confidence intervals. In the Cox analysis, exp (β) was the hazard ratio for a case with the characteristic, as compared to a case without the characteristic. For all analyses, $P < 0.05$ was considered statistically significant. StatView 5.0 statistical software (Abacus Concepts, Inc., Berkeley, CA, USA) was used for statistical analysis.

RESULTS

Baseline characteristics

Forty-eight patients underwent tonsillectomy and 70 patients did not before or after renal biopsy. The mean duration of follow-up for the 118 IgAN patients with and without tonsillectomy was 192.9 ± 74.8 months (median, 189.5 months; range, 48 to 326 months). The mean follow-up periods in the tonsillectomy and nontonsillectomy groups were 210.2 ± 78.9 months and 180.1 ± 70.0 months, respectively. The amount of urine protein excretion in 45 (38.1%) of 118 patients was less than 0.5 g/24 hours. Thirty-nine (33.1%) patients presented with macrohematuria at the time of renal biopsy. Baseline clinical and laboratory data at the time of renal biopsy were not statistically different between the tonsillectomy and nontonsillectomy groups (Table 1).

The damage severity of renal biopsy tissue, including glomerulus, interstitium, and vessels, was examined with light microscopy and was evaluated semiquantitatively. The comparison of renal biopsy pathologic findings between the tonsillectomy and nontonsillectomy groups was not statistically different (Table 1). Arterial sclerosis and adhesion were not statistically different either (data not shown).

The medical therapies included steroid, immunosuppressive, antiplatelet, and antihypertensive agents. Twenty-seven patients with tonsillectomy and 32 patients without tonsillectomy did not undergo any drug therapy during follow-up. The treatments in the tonsillectomy and nontonsillectomy groups were not significantly different (Table 1).

Clinical outcomes

One (2.1%) of the tonsillectomy patients and two (2.9%) of the nontonsillectomy patients died due to an accident, bacterial infection, and cerebral hemorrhage, respectively, before renal failure. The mortality in the tonsillectomy and nontonsillectomy groups was not significantly different (Fig. 1).

Five (10.4%) of 48 patients with tonsillectomy reached

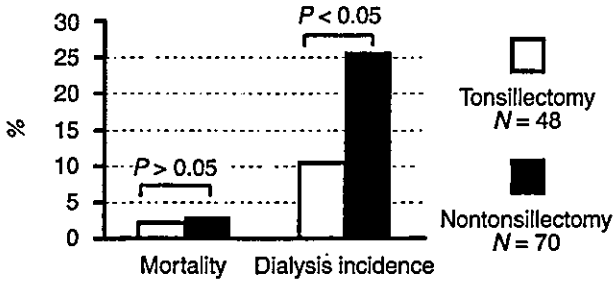

Fig. 1. Comparison of mortality before renal failure and incidence of dialysis event in the tonsillectomy and nontonsillectomy groups.

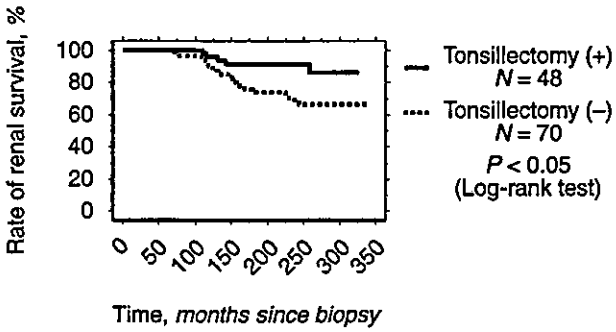

Fig. 2. Kaplan-Meier analysis of renal survival (dialysis-free) in immunoglobulin A nephropathy (IgAN) patients with (+) and without (–) tonsillectomy. The rates of renal survival in IgAN patients with and without tonsillectomy were 97.6%, 89.6%, 89.6%, 83.2%, and 88.8%, 74.0%, 63.7%, and 63.7% 120, 180, 240, and 300 months after renal biopsy, respectively.

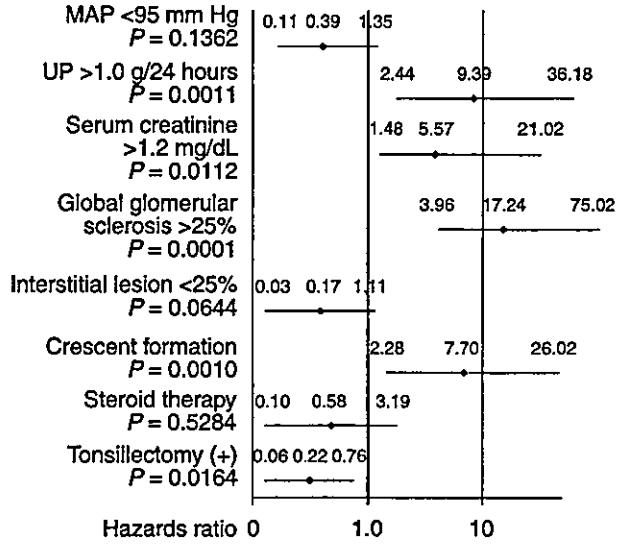

Fig. 3. Hazard ratios for the Cox regression model in immunoglogulin A nephropathy (IgAN). Numbers are hazard ratios with 95% confidence intervals (0.95% CI). Global glomerular sclerosis, crescent formation, a large amount of urine protein excretion, and elevated serum creatinine were statistically significant risk factors for renal prognosis. Conversely, tonsillectomy showed a favorable effect on renal prognosis. Abbreviations are: MAP, mean arterial pressure; UP, urine protein excretion.

the end point and required dialysis therapy, whereas 18 (25.7%) of 70 patients without tonsillectomy required dialysis therapy. Between the two groups there was a significant difference ($\chi^2 = 4.246$, $P = 0.0393$) (Fig. 1).

Renal survival in patients with and without tonsillectomy

The mean renal survival time and cumulative renal survival rate were evaluated by Kaplan-Meier analysis. The mean renal survival time was 243.8 months (standard error 7.0), and the cumulative renal survival rates were 97.6%, 89.6%, 89.6%, and 83.2% at 120, 180, 240, and 300 months, respectively, in the patients with tonsillectomy. In the patients without tonsillectomy, the mean renal survival time was 213.7 months (standard error 6.6), and the cumulative renal survival rates were 88.8%, 74.0%, 63.7%, and 63.7% at the 120, 180, 240, and 300 months, respectively. In the log-rank test, there was a significant difference between the two groups ($P = 0.0329$) (Fig. 2).

Cox regression analysis

Multivariate Cox regression analysis with the eight most important clinicopathologic variables (potential impact factors for renal prognosis) revealed that global glomerular sclerosis, crescent formation, a high amount of urine protein excretion, and elevated serum creatinine to be statistically significant risk factors for renal prognosis. Conversely, tonsillectomy was found to have a favorable effect on renal prognosis (Fig. 3).

Comparison of tonsillectomy patients requiring or not requiring dialysis

In order to further understand the renal indication and efficiency or limitations of tonsillectomy, we compared the baseline characteristics and histopathologic findings of 48 tonsillectomy IgAN patients with and without dialysis. As a result, the amount of urinary protein excretion at the time of renal biopsy and grades of global glomerular sclerosis and crescent formation in five patients requiring dialysis were significantly higher than those in 43 patients not requiring dialysis (2.04 ± 2.24 g/24 hours vs. 0.77 ± 0.86 g/24 hours, $P = 0.0155$; 1.60 ± 1.52 vs. 0.67 ± 0.81, $P = 0.0343$; and 1.40 ± 0.89 vs. 0.33 ± 0.53, $P = 0.0003$, respectively) (Fig. 4).

Comparison of tonsillectomy efficacy under different conditions

With a mild renal injury condition, where the amount of urine protein excretion was less than 1.0 g/24 hours and global glomerular sclerosis less than 25%, none of 26 patients with tonsillectomy needed dialysis, whereas five (13.2%) of 38 patients without tonsillectomy re-

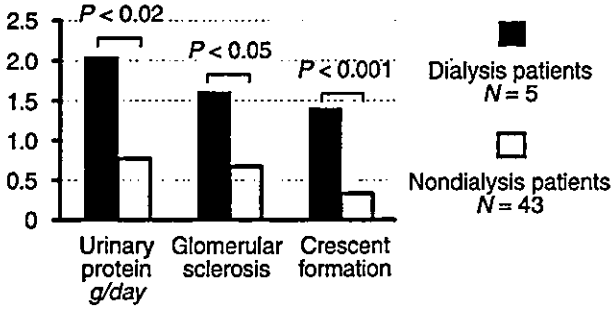

Fig. 4. Comparison of main baseline characteristics in tonsillectomy patients requiring or not requiring dialysis. The grades of global glomerular sclerosis and crescent formation were defined as 0 = no lesion; 1 = <25% of the lesion range; 2 = ≥25% and <50%, respectively.

quired dialysis. The percent requiring dialysis in the tonsillectomy patients with moderate renal injury was less than half of that in the nontonsillectomy patients, although there was no statistical difference between the two groups. On the other hand, in the patients with marked renal injury, tonsillectomy had no distinct effect on renal outcome (Table 2).

DISCUSSION

In the present study, we investigated the impact of tonsillectomy on long-term renal survival in patients with IgAN. There were two characteristics in this study. First, to our knowledge, the present study had the longest follow-up time, with a mean follow-up duration of more than 15 years (192.9 ± 74.8 months) on the efficacy of tonsillectomy in IgAN patients. Second, the end point of the observation in this study was from the time requiring dialysis, that is, renal death, not the time of a 50% increase in baseline serum creatinine. Although the end point of observation in the study by Rasche, Schwarz, and Keller [15] was also end-stage renal failure, the mean observation time after renal biopsy was only 3.4 ± 4 years. It is difficult to assess the real prognosis of patients with IgAN with a short observation time of less than 5 years, because only a small proportion of them enter dialysis treatment within 5 years [3, 16, 17].

Regarding the impact of tonsillectomy on progression and prognosis of IgAN, previous studies have demonstrated that tonsillectomy improves immunologic abnormalities, urinary abnormalities, renal function, and renal histopathologic findings in patients with IgAN (detailed in the next section). This study showed that tonsillectomy was an independent favorable factor on long-term renal survival in patients with IgAN.

Bene et al [18] reported that the serum IgA level and amount of urinary protein excretion significantly decreased, while serum creatinine concentration was stable, in patients with IgAN from 6 months to more than 4 years after tonsillectomy. Remission of proteinuria was observed in 41.7% of patients 6 months after tonsillectomy and in 50.0% 2 years after the surgery [13]. The clinical remission rate and stable renal function rate in IgAN patients with tonsillectomy were significantly higher than those in nontonsillectomy patients [19]. Hotta et al [14] conducted a retrospective investigation of the renal outcome in IgAN patients with a median observation period of 75 months after tonsillectomy and steroid pulse therapy. Their results showed that there were no significant differences between the tonsillectomy and nontonsillectomy groups regarding the incidence of progressive renal functional loss, defined as a 50% increase in baseline serum creatinine, but a combination of tonsillectomy and steroid pulse therapy had a significant impact on clinical remission by multivariate Cox regression analysis. Forty-eight percent of patients achieved clinical remission (disappearance of urinary abnormalities) and none of these remission patients revealed a progressive deterioration in renal function, defined as a 50% increase in the serum creatinine level from the baseline [14]. Thirty-five patients with IgAN, in whom hematuria had disappeared after a treatment protocol involving high doses of methylprednisolone and tonsillectomy, underwent a repeat biopsy; mesangial proliferation and acute inflammatory glomerular lesions, renal interstitial injury, and IgA mesangial deposits were significantly reduced in second-biopsy specimens [20]. In the present study, we used three different statistical methods including the chi-square test, Kaplan-Meier method with log-rank test, and Cox regression proportional hazards model in order to establish the efficacy of tonsillectomy in IgAN patients. A mean 15 years after a diagnostic biopsy, only five (10.4%) of 48 tonsillectomy patients entered dialysis, whereas 18 (25.7%) of 70 nontonsillectomy patients required dialysis, by chi-square test, $P = 0.0393$. Kaplan-Meier analysis showed the renal survival rates of tonsillectomy patients were statistically higher than those of nontonsillectomy ones 10, 15, 20, and 25 years after renal biopsy, respectively (log-rank test, $P = 0.0329$). Cox regression analysis showed that the relative risk for terminal renal failure in patients with tonsillectomy was lower compared to nontonsillectomy patients ($P = 0.0164$). The results of these three statistical analyses were consistent: all revealed that tonsillectomy had a favorable effect on long-term renal survival in patients with IgAN.

Although the mechanism regarding the favorable effect of tonsillectomy on renal survival in IgAN patients is still unclear, previous studies have suggested that the tonsils are closely related to IgAN. IgAN is initiated by glomerular deposition of polymeric IgA1. Tomino et al [21] demonstrated that the antibodies eluted from renal tissues of IgAN specifically bound with the nuclear regions of tonsillar cells. The binding of eluted antibodies

Table 2. Comparison of tonsillectomy efficacy under different conditions

	Tonsillectomy	Nontonsillectomy
Mild renal injury		
Urine protein <1 g/24 hours and global glomerular sclerosis grade ≤1	0/26 (0.0%)	5/38 (13.2%)
Moderate renal injury		
Urine protein ≥1 g/24 hours	4/16 (25.0%)	12/22 (54.5%)
Global glomerular sclerosis grade 2	2/6 (33.3%)	9/13 (69.2%)
Crescent formation grade 1	4/16 (25.0%)	9/17 (52.9%)
Marked renal injury		
Urine protein ≥1 g/24 hours and global glomerular sclerosis grade 2	1/2 (50.0%)	8/10 (80.0%)
Urine protein ≥1 g/24 hours and crescent formation grade 1	3/7 (42.9%)	5/9 (55.6%)
Crescent formation grade 2	3/4 (75.0%)	4/4 (100.0%)

Numbers refer to numbers of patients requiring dialysis. Although there was no statistical difference between the two groups, the percentage entering dialysis in the tonsillectomy patients with mild or moderate renal injury was less than half of that in the nontonsillectomy patients. Renal tissue injury grade ≤1 includes 0 and 1; grade 1 = ≥1% and <25%, grade 2 = ≥25% and <50%.

and tonsillar cells was completely inhibited by the addition of antihuman IgA antisera [21]. In tonsils without IgAN, the predominance of IgG-secreting cells was observed, while in IgAN patients, abnormal numbers of IgA-producing cells could be found in the tonsillar tissue, resulting in an inverted IgG/IgA ratio. Moreover, most IgA-producing cells were polymeric IgA-secreting cells (J chain-positive) [22–25]. A further study showed that the IgA1 subclass was demonstrated in follicular dendritic cells of the tonsils in IgAN patients, but not in the cells of non-IgAN controls [26]. A greater number of J chain mRNA-positive cells were found in the tonsillar germinal centers of IgAN patients compared with controls [27]. These results indicate that the polymeric IgA1 deposited in the mesangium may be at least in part of tonsillar origin. In addition, recurrent tonsillitis appears as the most frequent extrarenal clinical manifestation occurring in IgAN [28], and there are close time relationships between pharyngeal infectious episodes and bouts of hematuria and/or proteinuria [18]. Suzuki et al [29] reported that the antigens and antibodies of outer membranes of *Haemophilus parainfluenzae*, a common bacterium on the tonsils, were present in the glomerular mesangium and sera of IgAN, respectively [29]. Tonsillar lymphocytes from patients with IgAN had a significantly higher stimulation index on exposure to *H. parainfluenzae* antigens and a significantly higher IgA stimulation index than did controls [30]. Tonsillectomy could thus lead to the disappearance of lymphoid tissue actively recruiting activated IgA-producing cells and the removal of a pharyngeal infectious focus, and explain partly the decrease in serum IgA level and mesangial IgA deposits, and subsequent remission in IgAN.

Regarding the limitations and indication of tonsillectomy in patients with IgAN, our data (Fig. 4 and Table 2) suggested that when the amount of urine protein excretion was more than 1.0 g/24 hours and global glomerular sclerosis was greater than 25%, or crescent formation was greater than 25%, patients could develop renal failure requiring dialysis even if tonsillectomy was performed. Tonsillectomy was mainly indicated for patients with mild IgAN, in which the amount of urine protein excretion was less than 1.0 g/24 hours and global glomerular sclerosis was less than 25%.

Although this study was performed in a retrospective style, we believe the clinical and histologic data of the baseline and the outcomes of end points are precise, because follow-up after renal biopsy was done annually with accurate records. The long observation periods enabled us to obtain results showing a significant difference in the incidence of renal death over 15 years after tonsillectomy. Although randomized prospective controlled trials are very important, a randomized control study of a surgical operation such as tonsillectomy is hard to perform, and long-term follow up more than 10 years is not easy. Therefore, even if the bias as a result of retrospective study is taken into account, we believe this study will have referential value for clinicians. Unfortunately, we could not accurately measure drug dosage or continual time of medical therapies during the clinical course in this study. Although we have detailed therapy protocols on IgAN at present, there were no detailed treatment plans two decades ago. Only a small fraction of patients underwent medical therapy in this study. One possible explanation is that the prognosis of IgAN was initially considered to be favorable [31]. According to the policy two decades ago, many patients with mild IgAN were not given any agents after diagnosis.

CONCLUSION

The results of this study showed tonsillectomy had a favorable effect on long-term renal survival in patients with IgAN. Since no specific method has been available for the treatment of IgAN, tonsillectomy could be used as a potentially effective treatment, especially in patients with mild IgAN. However, tonsillectomy may not be enough, because of multiple related factors in the progression in patients with IgAN, including genetic factors [32–35]. In IgAN patients with marked renal injury, ton-

sillectomy may not affect the prognosis of IgAN. In order to further clarify the clinical efficacy of tonsillectomy, randomized prospective controlled trials are necessary.

ACKNOWLEDGMENTS

This work was supported by a Health and Labor Science Research Grant for Research on Specific Diseases from the Ministry of Health, Labor and Welfare (to Fumitake Gejyo). The authors thank all colleagues who took medical records, performed renal biopsies and tonsillectomy operation, did histopathologic diagnoses, and who assisted with follow-up. An abstract of this work was presented at the 26th International Congress of Internal Medicine (Kyoto, Japan, 2002).

Reprint requests to Fumitake Gejyo, Division of Clinical Nephrology and Rheumatology, Niigata University Graduate School of Medical and Dental Sciences, 1-757 Asahimachi-dori, Niigata 951- 8510, Japan.
E-mail: gejyo@med.niigata-u.ac.jp

REFERENCES

1. Nishi S: The prognosis of IgA nephropathy—favorable or poor? *Intern Med* 40:679–680, 2001
2. Stratta P, Segoloni GP, Canavese C, *et al*: Incidence of biopsy-proven primary glomerulonephritis in an Italian province. *Am J Kidney Dis* 27:631–639, 1996
3. Koyama A, Igarashi M, Kobayashi M: Natural history and risk factors for immunoglobulin A nephropathy in Japan. Research Group on Progressive Renal Diseases. *Am J Kidney Dis* 29:526–532, 1997
4. D'Amico G, Imbasciati E, Barbiano Di Belgioioso G, *et al*: Idiopathic IgA mesangial nephropathy. Clinical and histological study of 374 patients. *Medicine (Baltimore)* 64:49–60, 1985
5. Schena FP: A retrospective analysis of the natural history of primary IgA nephropathy worldwide. *Am J Med* 89:209–215, 1990
6. Pettersson E: IgA nephropathy: 30 years on. *J Intern Med* 242:349–353, 1997
7. Szeto CC, Lai FM, To KF, *et al*: The natural history of immunoglobulin A nephropathy among patients with hematuria and minimal proteinuria. *Am J Med* 110:434–437, 2001
8. Tomino Y: IgA nephropathy. From molecules to men. *Contrib Nephrol* 126:1–115, 1999
9. Ballardie FW, Roberts IS: Controlled prospective trial of prednisolone and cytotoxics in progressive IgA nephropathy. *J Am Soc Nephrol* 13:142–148, 2002
10. Donadio JV Jr, Bergstralh EJ, Offord KP, *et al*: A controlled trial of fish oil in IgA nephropathy. Mayo Nephrology Collaborative Group. *N Engl J Med* 331:1194–1199, 1994
11. Masuda Y, Terazawa K, Kawakami S, *et al*: Clinical and immunological study of IgA nephropathy before and after tonsillectomy. *Acta Otolaryngol* (Suppl 454):248–255, 1988
12. Tamura S, Masuda Y, Inokuchi I, *et al*: Effect of and indication for tonsillectomy in IgA nephropathy. *Acta Otolaryngol* (Suppl 508):23–28, 1993
13. Akagi H, Nishizaki K, Hattori K, *et al*: Prognosis of tonsillectomy in patients with IgA nephropathy. *Acta Otolaryngol* (Suppl 540):64–66, 1999
14. Hotta O, Miyazaki M, Furuta T, *et al*: Tonsillectomy and steroid pulse therapy significantly impact on clinical remission in patients with IgA nephropathy. *Am J Kidney Dis* 38:736–743, 2001
15. Rasche FM, Schwarz A, Keller F: Tonsillectomy does not prevent a progressive course in IgA nephropathy. *Clin Nephrol* 51:147–152, 1999
16. Bailey RR, Lynn KL, Robson RA, *et al*: Long term follow up of patients with IgA nephropathy. *N Z Med J* 107:142–144, 1994
17. Wyatt RJ, Kritchevsky SB, Woodford SY, *et al*: IgA nephropathy: Long-term prognosis for pediatric patients. *J Pediatr* 127:913–919, 1995
18. Bene MC, Hurault de Ligny B, Kessler M, *et al*: Tonsils in IgA nephropathy. *Contrib Nephrol* 104:153–161, 1993
19. Kosaka M: Long-term prognosis for tonsillectomy patients with IgA nephropathy. *Nippon Jibiinkoka Gakkai Kaiho* 101:916–923, 1998
20. Hotta O, Furuta T, Chiba S, *et al*: Regression of IgA nephropathy: A repeat biopsy study. *Am J Kidney Dis* 39:493–502, 2002
21. Tomino Y, Sakai H, Endoh M, *et al*: Cross-reactivity of IgA antibodies between renal mesangial areas and nuclei of tonsillar cells in patients with IgA nephropathy. *Clin Exp Immunol* 51:605–610, 1983
22. Bene MC, Faure G, Hurault de Ligny B, *et al*: Immunoglobulin A nephropathy. Quantitative immunohistomorphometry of the tonsillar plasma cells evidences an inversion of the immunoglobulin A versus immunoglobulin G secreting cell balance. *Clin Invest* 71:1342–1347, 1983
23. Egido J, Blasco R, Lozano L, *et al*: Immunological abnormalities in the tonsils of patients with IgA nephropathy: inversion in the ratio of IgA: IgG bearing lymphocytes and increased polymeric IgA synthesis. *Clin Exp Immunol* 57:101–106, 1984
24. Nagy J, Brandtzaeg P: Tonsillar distribution of IgA and IgG immunocytes and production of IgA subclasses and J chain in tonsillitis vary with the presence or absence of IgA nephropathy. *Scand J Immunol* 27:393–399, 1988
25. Bene MC, Hurault De Ligny B, Kessler M, Faure GC: Confirmation of tonsillar anomalies in IgA nephropathy: a multicenter study. *Nephron* 58:425–428, 1991
26. Kusakari C, Nose M, Takasaka T, *et al*: Immunopathological features of palatine tonsil characteristic of IgA nephropathy: IgA1 localization in follicular dendritic cells. *Clin Exp Immunol* 95:42–48, 1994
27. Harper SJ, Allen AC, Bene MC, *et al*: Increased dimeric IgA-producing B cells in tonsils in IgA nephropathy determined by in situ hybridization for J chain mRNA. *Clin Exp Immunol* 101:442–448, 1995
28. Caraman PL, Azoulay E, Kessler M, *et al*: Mucosal infections and allergy in IgA nephropathy. A retrospective study. *Contrib Nephrol* 104:24–30, 1993
29. Suzuki S, Nakatomi Y, Sato H, *et al*: *Haemophilus parainfluenzae* antigen and antibody in renal biopsy samples and serum of patients with IgA nephropathy. *Lancet* 343:12–16, 1994
30. Suzuki S, Fujieda S, Sunaga H, *et al*: Synthesis of immunoglobulins against *Haemophilus parainfluenzae* by tonsillar lymphocytes from patients with IgA nephropathy. *Nephrol Dial Transplant* 15:619–624, 2000
31. van der Peet J, Arisz L, Brentjens JR, *et al*: The clinical course of IgA nephropathy in adults. *Clin Nephrol* 8:335–340, 1977
32. Gejo F, Shimada H, Ueno M, *et al*: Clinical aspect of IgA nephropathy. *Nippon Naika Gakkai Zasshi* 89:1935–1941, 2000
33. Galla JH: Molecular genetics in IgA nephropathy. *Nephron* 88:107–112, 2001
34. Narita I, Saito N, Goto S, *et al*: Role of uteroglobin G38A polymorphism in the progression of IgA nephropathy in Japanese patients. *Kidney Int* 61:1853–1858, 2002
35. Goto S, Narita I, Saito N, *et al*: A (-20) C polymorphism of angiotensinogen gene and the progression of IgA nephropathy. *Kidney Int* 62:980–985, 2002

Kidney International, Vol. 64 (2003), pp. 2–10

GENETIC DISORDERS–DEVELOPMENT

Pathogenesis of nephrogenic diabetes insipidus by aquaporin-2 C-terminus mutations

Tomoki Asai, Michio Kuwahara, Hidetake Kurihara, Tatsuo Sakai, Yoshio Terada, Fumiaki Marumo, and Sei Sasaki

Department of Homeostasis Medicine and Nephrology, Tokyo Medical and Dental University Graduate School, Tokyo, Japan; and Department of Anatomy, Juntendo University School of Medicine, Tokyo, Japan

Pathogenesis of nephrogenic diabetes insipidus by aquaporin-2 C-terminus mutations.

Background. We previously reported three aquaporin-2 (AQP2) gene mutations known to cause autosomal-dominant nephrogenic diabetes insipidus (NDI) (*Am J Hum Genet* 69: 738, 2001). The mutations were found in the C-terminus of AQP2 (721delG, 763 to 772del, and 812 to 818del). The wild-type AQP2 is a 271 amino acid protein, whereas these mutant genes were predicted to encode 330 to 333 amino acid proteins due to the frameshift mutations leading to the creation of a new stop codon 180 nucleotides downstream. The *Xenopus* oocyte expression study suggested that the trafficking of the mutant AQP2s was impaired.

Methods. To determine the cellular pathogenesis of these NDI-causing mutations in mammalian epithelial cells, Madin-Darby canine kidney (MDCK) cells were stably transfected with the wild-type AQP2, or the 763 to 772del mutant AQP2, or both. Cells were grown on the membrane support to examine the localization of AQP2 proteins by immunofluorescence microscopy.

Results. Confocal immunofluorescence microscopy showed that the wild-type AQP2 was expressed in the apical region, whereas the mutant AQP2 was apparently located at the basolateral region. Furthermore, the wild-type and mutant AQP2s were colocalized at the basolateral region when they were cotransfected, suggesting the formation of mixed oligomers and thereby mistargeting.

Conclusion. Mixed oligomers of the wild-type and the 763 to 772del mutant AQP2s are mistargeted to the basolateral membrane due to the dominant-negative effect of the mutant. This defect is very likely to explain the pathogenesis of autosomal-dominant NDI. The mistargeting of the apical membrane protein to the basolateral membrane is a novel molecular pathogenesis of congenital NDI.

By current consensus, aquaporin-2 (AQP2) is known as a vasopressin-regulated water channel confined to the collecting duct cells [1]. There is accumulating evidence that the binding of vasopressin to the V2 receptor at the basolateral membrane initiates intracellular signaling cascades, leading to redistribution of AQP2 from the subapical intracellular vesicle to the apical membrane [2, 3]. Congenital nephrogenic diabetes insipidus (NDI) is a hereditary disease characterized by a lack of responsiveness to vasopressin in the renal collecting tubule. The majority of NDI patients develop the disease due to mutations in the *AVPR2* gene and manifested a pattern of X-linked recessive inheritance [2, 3]. In the autosomal-recessive form of NDI, mutations were detected in the *AQP2* gene [4].

In a recent study, a point mutation (E258K) causing the autosomal-dominant form of NDI was identified in one allele in exon 4 of the *AQP2* gene [5]. This E258K-AQP2 mutant heterotetramerize with the wild-type AQP2, but these tetramers retained in the Golgi compartment in the *Xenopus* oocyte, suggesting that the dominant-negative effect of the mutant causes the autosomal-dominant NDI [5, 6]. We also reported three mutations of the *AQP2* gene responsible for the autosomal-dominant form of NDI [7]. These mutations were also found in a single allele of the *AQP2* gene at the C-terminus: a deletion of G at 721 (721delG), a deletion of 10 nucleotides starting at 763 (763 to 772del), and a deletion of seven nucleotides starting at 812 (812 to 818del). Each of these mutations shifts the stop codon 180 nucleotides downstream. In contrast to the wild-type AQP2 encoding a 271 amino acid protein, these mutants encode 330 to 333 amino acid proteins. Interestingly, all three of these mutants share a common sequence of 61 amino acids at the C-terminal (GRQRPLRPRRTLVR PEAEGPTPSLLSRRSEVGPPAQSSCFLDVRAQAS AVSRRGGG CRREP). Our *Xenopus* oocyte expression study suggested two things: (*1*) that the wild-type and mutant AQP2 proteins form mixed tetramers; and (*2*) that the trafficking to the plasma membrane is impaired in the mixed tetramers due to the dominant-negative

Key words: vasopressin, autosomal-dominant, aquaporin-2.

Received for publication February 7, 2002
and in revised form September 28, 2002, and January 17, 2003
Accepted for publication February 14, 2003

effect of the mutant AQP2. More recently, another AQP2 mutation causing the autosomal-dominant NDI (727delG) was reported [8]. When the wild-type and 727delG AQP2s were cotransfected in Madin-Darby canine kidney (MDCK) cells, the hetero-oligomers of the two AQP2s were predominantly localized at late endosomes/lysosomes [8].

Because our previous study in the autosomal-dominant NDI was performed using *Xenopus* oocytes, a nonpolarized cell type, our findings may not necessarily hold true for mammalian polarized epithelial cells such as renal tubular cells. In this study, we established cell lines that stably express the wild-type AQP2 and one of the mutant AQP2s (763 to 772) to clarify the pathogenesis of our NDI cases. We chose MDCK cells for transfection and the study was focused on the intracellular localization of AQP2 proteins.

METHODS

Preparation of cDNA

The wild-type cDNA of human AQP2 (GenBank accession number NM000486) with a Kozak consensus translation initiation site just upstream of the initial codon (ATG) was inserted into the pcDNA3.1 vector (Invitrogen, CH Groningen, The Netherlands) between the *Hin*dIII site and *Xba*I site. The splicing overlap extension polymerase chain reaction (PCR) technique [9] was used to delete 10 nucleotides starting at 763 from the cDNA of the wild-type human AQP2. In the first PCR step, the template AQP2 DNA was amplified using a 5′ initiation site primer (5′-CCCAAGCTTGCCGCCACCATGTGGGAGCTCCGCTCCATA-3′; underlining and double underlining denote the *Hin*dIII site and Kozak consensus translation initiation site, respectively), an antisense mutation primer (5′-AGGCTCTGCGGCGAGTGCAGCTCCGCCGTCGCA-3′; underlining denotes nucleotides at 752 to 762), a sense mutation primer (5′-GAGCGCGAGGTGCGACGGCGGAGCTGCACTCGC-3′; underlining denotes nucleotides at 773 to 784), and a 3′ end site primer (5′-CCCTCTAGATCAGGGCTCCCTCCGGCAGCC-3′; underlining denotes the *Xba*I site). In the second PCR step, DNA fragment of the 763 to 772del AQP2 was produced by PCR using the 5′ initiation site primer, the 3′ end site primer, and the two first PCR products as templates. The PCR products were digested with *Hin*dIII and *Xba*I, and inserted into the pcDNA3.1/Zeo vector (Invitrogen).

Cell culture and stable transfection

MDCK cells (Japanese Collection of Research Biologicals #9029) were cultured in Dulbecco's modified Eagle's medium (DMEM) (Gibco BRL, Grand Island, NY, USA) supplemented with 10% fetal bovine serum (FBS), 100 U/mL of penicillin, and 100 μg/mL of streptomycin. Cells were grown at 37°C under a humidified 5% CO_2 atmosphere. Ten micrograms of the expression constructs of the wild-type AQP2 and the 763 to 772del mutant were transfected into MDCK cells grown subconfluently on dishes (90 mm in diameter) using the calcium-phosphate precipitation technique. After 24 hours, the cells transfected with the wild-type AQP2 and the mutant AQP2 were trypsinized, split among six dishes, and cultured in DMEM containing 700 μg/mL of G418 (Sigma Chemical Co., St. Louis, MO, USA) and 400 μg/mL of Zeocin (Invitrogen), respectively. Ten to fourteen days after the transfection, individual colonies were selected using cloning rings and expanded. Native vectors were also transfected into MDCK cells as controls. To establish the cotransfected cells, the mutant AQP2 was transfected into the cells stably expressing wild-type AQP2 and cultured in DMEM containing G418 and Zeocin. After the selection, the clones were isolated.

Immunoblot analysis

Transfected cells were homogenized for 30 minutes in RIPA buffer [50 mmol/L Tris-HCl, 150 mmol/L NaCl, 1.0% NP40, 0.5% deoxycholate, 0.1% sodium dodecyl sulfate (SDS), pH 8.0] containing a protease inhibitor cocktail (Boehringer Manheim, Manheim, Germany). The cell lysate was centrifuged at 10,000*g* at 4°C for 30 minutes. The supernatant was denatured in SDS sample buffer at 70°C for 10 minutes. Ten micrograms of total membrane protein were loaded in each lane. The samples were separated by SDS polyacryamide gel electrophoresis (PAGE) and transferred to Immobilon-P filters (Millipore, Bedford, MA, USA) using a semidry system. After blocking the filters overnight in 2% skim milk in TBST solution (20 mmol/L Tris, 150 mmol/L NaCl, 0.05% Triton-X, pH 7.4), they were incubated for 1 hour with either an affinity-purified rabbit antibody against 15 carboxy terminal amino acids of the wild-type or an affinity-purified rat antibody against 15 carboxy terminal amino acids of the mutant AQP2. The filters were then incubated for an additional 1 hour with ^{125}I-protein A solution and examined by autoradiography.

For immunoprecipitation, the membrane fraction of MDCK cells was obtained as described above. Fifty micrograms of the membrane protein were incubated with an antibody against the wild-type or mutant AQP2 for 2 hours at 4°C. Then, protein G agarose (Protein G PLUS-Agarose, Oncogene Science, Uniondale, NY, USA) was added to each sample and incubated for 12 hours at 4°C. After three washes, the samples were denatured, separated by SDS-PAGE, and treated by methods similarly to those described above.

Immunofluorescence microscopy

To detect the localization of proteins in polarized cells, transfected MDCK cells were grown on a permeable supported membrane (Transwell-Clear, Corning, Cambridge, MA, USA). After the 3-day culture in DMEM,

confluent cells were incubated for 2 hours with DMEM containing 10^{-5} mol/L forskolin (Sigma Chemical Co.) to induce the expression of AQP2 to the plasma membrane. In some protocols, cells were not treated with forskolin for comparison. The cells were then fixed for 20 minutes with 2% paraformaldehyde in serum-free DMEM at room temperature, washed with phosphate-buffered saline (PBS), permeabilized with 0.2% Triton X-100 in PBS, blocked with 1% bovine serum albumin (BSA) in PBS at 4°C overnight, and doubly stained. Antibodies against the following proteins were used: the wild-type AQP2 (rabbit or rat, diluted 1:1200), the mutant AQP2 (rabbit, 1:600), a tight junction protein, ZO-1 (mouse, 1:400) (Zymed Laboratories, South San Francisco, CA, USA), a basolateral membrane marker protein, Na-K-ATPase (mouse, 1:400) (Upstate Biotechnology, Lake Placid, NY, USA), and a late endosomal/lysosomal marker protein known as lysosome-associated membrane protein 1 (Lamp1; rabbit, 1:200, kindly provided by Dr. E. Kominami). Cells transfected with the wild-type or the mutant AQP2 were incubated at room temperature for 1 hour with the mixture of two antibodies in PBS containing 1% BSA. After four washes with PBS, the cells were further incubated with a fluorescence-labeled antibody against rabbit immunoglobulin G (IgG) (1:200) (Alexa Fluor 488, Molecular Probes, Eugene, OR, USA), or rat or mouse IgG (1:200) (Alexa Fluor 568, Molecular Probes) for 1 hour. Mock-transfected cells were treated similarly to provide control. After staining, the cells were washed four times with PBS and mounted in a mounting medium (Prolong Antifade Kit, Molecular Probes). Immunofluorescent images of horizontal or vertical sections were obtained with an LSM510 laser scanning confocal microscope system (Carl Zeiss, Jena, Germany) using a 60× water-immersion objective.

To examine the cross reactivity of antibodies against the mutant AQP2 (rabbit) and Na-K-ATPase (mouse), cells transfected with the mutant AQP2 were incubated with antimutant-AQP2 antibody, and then incubated with antibodies against rabbit or mouse IgG. In addition, the same cells were incubated with anti-Na-K-ATPase antibody, and then incubated with anti-mouse or rabbit IgG. The cross reactivity of antibodies against the wild-type AQP2 (rabbit) and Na-K-ATPase (mouse), and the wild-type AQP2 (rat) and mutant AQP2 (rabbit) were tested similarly.

RESULTS

The apparent molecular sizes of the wild-type AQP2 and mutant AQP2 corresponded to 29 kD and 34 kD, respectively [7]. Immunoblots of MDCK cells transfected with the wild-type AQP2 (Fig. 1A) and the mutant AQP2 (Fig. 1B) revealed clear bands at 29 kD and 34 kD, respectively, and broad glycosylated bands at 40 to 50 kD. In contrast, no bands were seen in mock-transfected cells (Fig. 1 A and B). In the immunoblots of cotransfected cells (Fig. 1C), the mixture of two antibodies revealed both 29 kD and 34 kD bands at similar expression levels. These results suggested that the wild-type and/or mutant AQP2s were successfully transfected in MDCK cells.

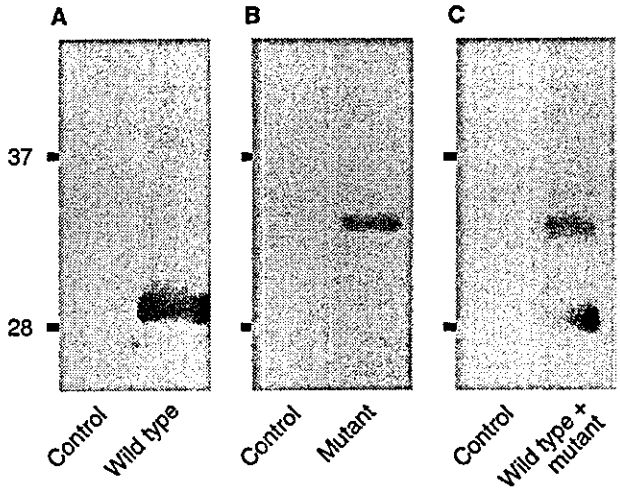

Fig. 1. Immunoblot of membrane fractions of the Madin-Darby canine kidney (MDCK) cells transfected with the wild-type aquaporin-2 (AQP2) (*A*), mutant AQP2 (*B*), and both wild-type and mutant AQP2s (*C*). The protein expression was detected with an affinity-purified antibody against the wild-type (A), mutant AQP2 (B), or a mixture of both (C).

The localization of proteins was examined in polarized MDCK cells by immunofluorescence microscopy. After incubation with forskolin, cells transfected with the wild-type AQP2 were doubly stained with antibodies against the wild-type AQP2 and ZO-1, a tight junction marker. The staining with anti-wild-type AQP2 antibody was almost homogenous in the XY section of each cell, and predominantly localized at the apical side in the XZ section (Fig. 2A). The staining with anti-ZO-1 antibody was found at the apical side of the cell outline, the localization compatible with that of the tight junction (Fig. 2B). The merged figure confirmed the apical distribution of the wild-type AQP2 (Fig. 2C). Figure 2 D and E shows the double staining of the wild-type AQP2 (green) and Na-K-ATPase (red), a basolateral membrane marker, in cells before and after forskolin treatment, respectively. The wild-type AQP2 was mainly distributed at the apical region even without incubation with forskolin (Fig. 2D). Forskolin apparently induced further redistribution of the wild-type AQP2 to the apical membrane (Fig. 2E), suggesting the stimulation of the apical trafficking of AQP2 by forskolin. In contrast to the AQP2-transfected

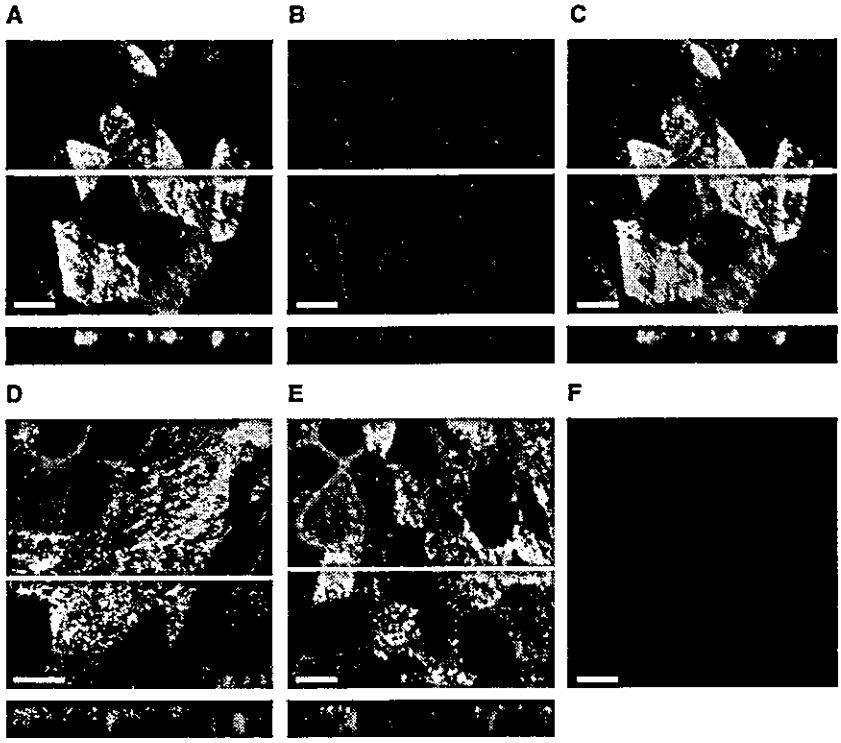

Fig. 2. Immunocytochemical localization of the wild-type aquaporin-2 (AQP2) in Madin-Darby canine kidney (MDCK) cells transfected with the wild-type AQP2 and mock-transfected MDCK cells. The samples were viewed with a confocal microscope at ×400. Localization of the wild-type AQP2 (*A*), ZO-1 (*B*), and merged (*C*). Localization of the wild-type AQP2 and Na-K-ATPase before (*D*) and after forskolin treatment (*E*). Mock-transfected cells (*F*) stained with antibody against the wild-type AQP2. XY and XZ sections are shown in the upper and lower panels, respectively. White bars indicate 10 μm.

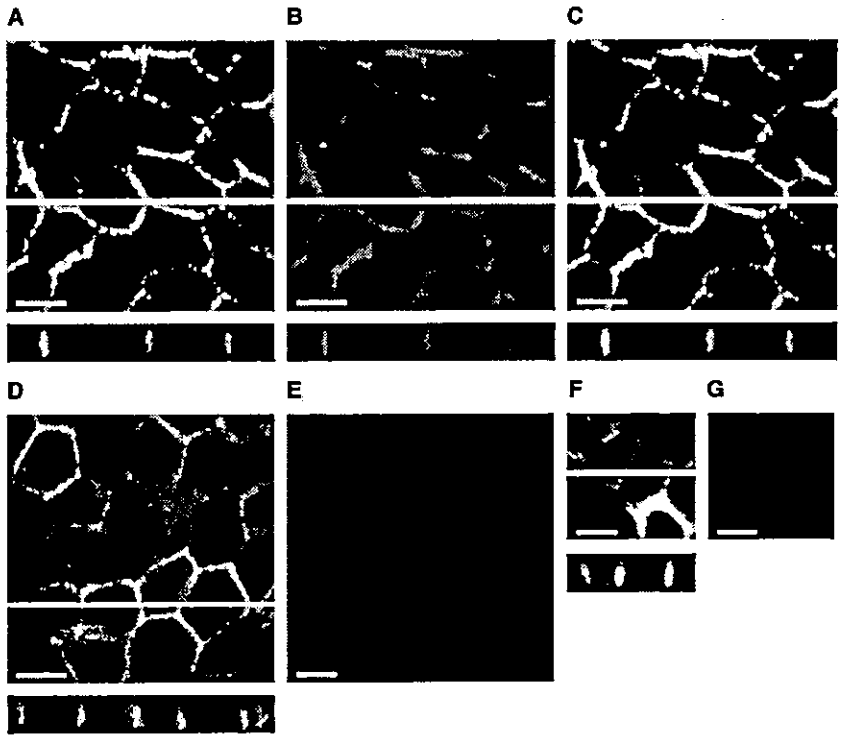

Fig. 3. Immunocytochemical localization of the mutant aquaporin-2 (AQP2) in Madin-Darby canine kidney (MDCK) cells transfected with the mutant AQP2 and mock-transfected MDCK cells. The samples were viewed at ×400X. Localization of the mutant AQP2 (*A*), Na-K-ATPase (*B*), merged with (*C*) or without forskolin treatment (*D*). In contrast to (A to C), the red and green fluorescence represent the staining of the mutant AQP2 and Na-K-ATPase, respectively, in (D). Mock-transfected cells stained with antibody against the mutant AQP2 (*E*). Determination of the cross-reactivity of antibodies. Cells were incubated with rabbit antimutant AQP2 antibody, and then incubated with antibodies against rabbit IgG (*F*) or mouse IgG (*G*). XY and XZ sections are shown in the upper and lower panels, respectively. White bars indicate 10 μm.

cells, no fluorescence from the AQP2 was visible in the mock-transfected cells (Fig. 2F).

In a preliminary study, we noted the conspicuous presence of the mutant AQP2 at the basolateral side. To investigate further, we doubly stained the cells transfected with the mutant AQP2 with antibodies against the mutant AQP2 and Na-K-ATPase after forskolin treatment. The lateral cell surface was brightly stained in the mutant AQP2-expressing cells, whereas the apical signal was negative (Fig. 3A). A weak staining of the basal cell membrane was also visible when the fluorescent image was turned up to high brightness on the monitor (figure not shown). A similar staining pattern was observed in Na-K-ATPase (Fig. 3B). The superimposition of these figures showed the colocalization of these two proteins (Fig. 3C), suggesting that the 763 to 772del mutation is responsible for the mistargeting of the AQP2 protein to the basolateral membrane area. Basolateral localization of the mutant AQP2 was also observed in cells not stimulated with forskolin (Fig. 3D). However, the colocalization of the mutant AQP2 and Na-K-ATPase were seemingly not so close as observed in forskolin-treated cells (Fig. 3C). In contrast to cells expressing the mutant AQP2, no fluorescence was detected in mock-transfected cells (Fig. 3E). Because Figure 3C showed a high overlap of two proteins, the cross-reactivity of two antibodies against the mutant AQP2 (rabbit) and Na-K-ATPase (mouse) was examined. Cells transfected with the mutant AQP2 were incubated with rabbit antimutant AQP2 antibody, and then incubated with anti-rabbit or mouse IgG. The mutant AQP2 was identified by the incubation with anti-rabbit IgG (Fig. 3F), but not with anti-mouse IgG (Fig. 3G), suggesting the cross-reactivity of these antibodies were not responsible for a close colocalization of the mutant AQP2 and Na-K-ATPase. When the same cells were pretreated with mouse anti-Na-K-ATPase antibody, anti-mouse IgG, but not anti-rabbit IgG, detected Na-K-ATPase (figures not shown), suggesting again absence of the cross-reaction.

Next, we examined the localization of the wild-type AQP2 and Na-K-ATPase in cells cotransfected with the wild-type and mutant AQP2s. After incubation with forskolin, the distribution of these proteins was similar to that observed in the mutant-transfected cells shown in Figure 3 (Fig. 4 A to C). The merged figure demonstrated colocalization of the wild-type AQP2 and Na-K-ATPase (Fig. 4C). When cells were preincubated with an antibody against the wild-type AQP2 (rabbit), the immunostaining of AQP2 was observed after incubation with anti-rabbit IgG (Fig. 4H), but not with anti-mouse IgG. (Fig. 4I), suggesting no cross-reactivity of these two antibodies. Similarly, the incubation with anti-mouse IgG, but not with anti-rabbit IgG, detected Na-K-ATPase in cells pretreated with mouse anti-Na-K-ATPase antibody (figures not shown). In general, AQPs are known to exist as tetramers at the plasma membrane. Therefore, we tested whether the wild-type and mutant AQP2s form oligomers by immunocytochemistry and immunoprecipitation. In cotransfected cells, double staining of the wild-type and mutant AQP2s showed a close localization (Fig. 4 D to F), suggesting the formation of mixed oligomers. The cross reaction of rat anti-wild-type AQP2 antibody and rabbit anti-mutant AQP2 antibody was excluded, because anti-rat IgG (Fig. 4J), but not anti-rabbit IgG (Fig. 4K), recognized the wild-type AQP2 in cells preincubated with anti-wild-type AQP2 antibody. Similarly, the mutant AQP2 was not identified by anti-rat IgG in cells preincubated with anti-mutant AQP2 antibody (figures not shown). When the membrane fractions of cotransfected cells were immunoprecipitated with an antibody against the wild-type AQP2, an antibody against the mutant AQP2 revealed a 34 kD band corresponding to the apparent molecular size of the mutant AQP2 (Fig. 5A). Furthermore, an anti-wild-type AQP2 antibody recognized a 29 kD band in the samples immunoprecipitated by an antimutant antibody (Fig. 5B), once more suggesting hetero-oligomerization. Taken together, our findings suggested that the mixed oligomers of the wild-type and mutant AQP2s were translocated to the basolateral surface, but not to the apical surface, due to the dominant-negative effect of the mutant.

Marr et al recently reported another AQP2 mutation in patients with autosomal-dominant NDI [8]. Their mutant (727delG) and our mutant (763 to 772del) share an identical C-terminal amino acids. They observed that the hetero-oligomer of the wild-type and 727delG AQP2s mainly localized to late endosomes/lysosomes in cotransfected cells [8]. Thus, we performed immunocytochemical studies in cells coexpressing the wild-type and 763-772del AQP2s. When cells were doubly stained with antibodies against ZO-1 and Lamp1, a marker of the late endosome/lysosome, fluorescence from Lamp1 was detected in the cytoplasm (Fig. 6 A to C). The cytoplasmic staining of Lamp1 was also seen in cells stained with antibodies against Na-K-ATPase and Lamp1 (Fig. 6 D to F). These findings suggested that the localization of Lamp1 seemed to differ from that of AQP2 hetero-oligomers that were essentially distributed at the basolateral membrane area (Fig. 4). Because both of our antibodies against the mutant AQP2 and Lamp1 were rabbit IgG, we were unable to detect the localization of these two proteins simultaneously in the present study.

DISCUSSION

The mutation of the mutant AQP2 used in this study is a deletion of 10 nucleotides starting at 763 (763 to 772del) in exon 4 of the *AQP2* gene [7]. The wild-type AQP2 is a 271 amino acid protein, whereas the 763 to 772del *AQP2* gene is predicted to encode 330 amino

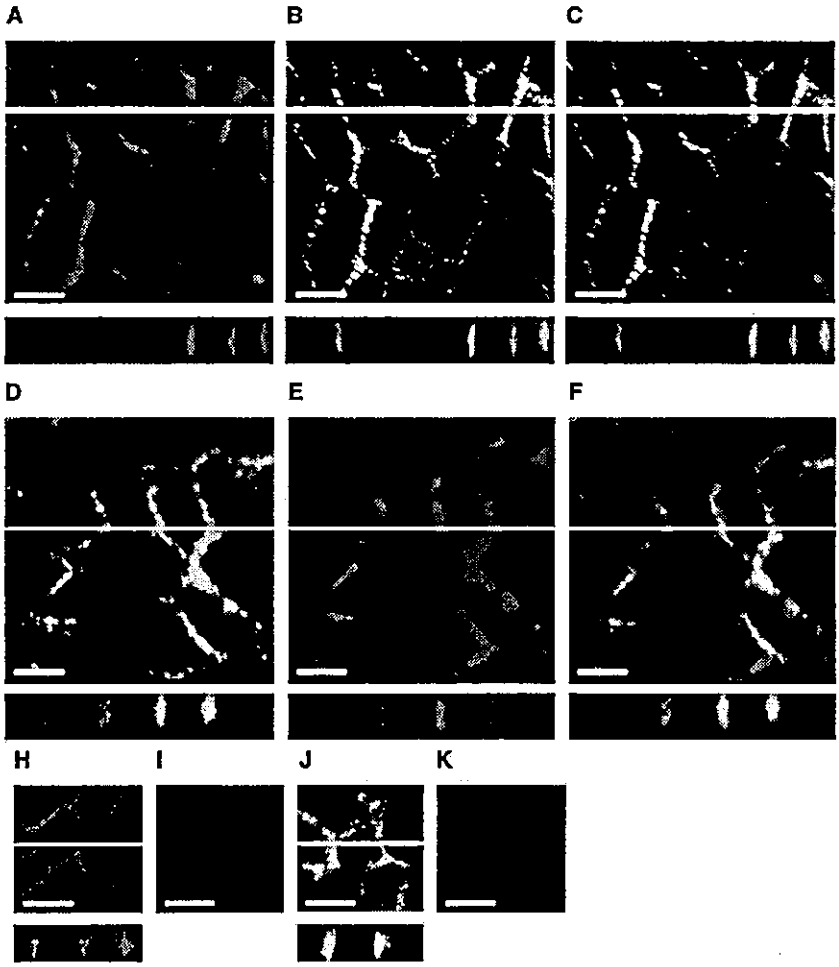

Fig. 4. Immunocytochemical localization of the wild-type and mutant aquaporin-2 (AQP2) in cotransfected Madin-Darby canine kidney (MDCK) cells. The wild-type and mutant AQP2s were stably cotransfected in MDCK cell. Colocalization of the wild-type AQP2 (*A*), Na-K-ATPase (*B*), and merged (*C*) was observed at ×400. Colocalization of the wild-type AQP2s (*D*), the mutant AQP2 (*E*), and merged (*F*) merged. Determination of the cross-reactivity of antibodies. Cells were incubated with rabbit anti-wild-type AQP2 antibody, and then incubated with antibodies against rabbit IgG (*H*) or mouse IgG (*I*). In addition, cells were incubated with rat anti-wild-type AQP2 antibody, and then incubated with antibodies against rat IgG (*J*) or rabbit IgG (*K*). XY and XZ sections are shown in the upper and lower panels, respectively. White bars indicate 10 μm.

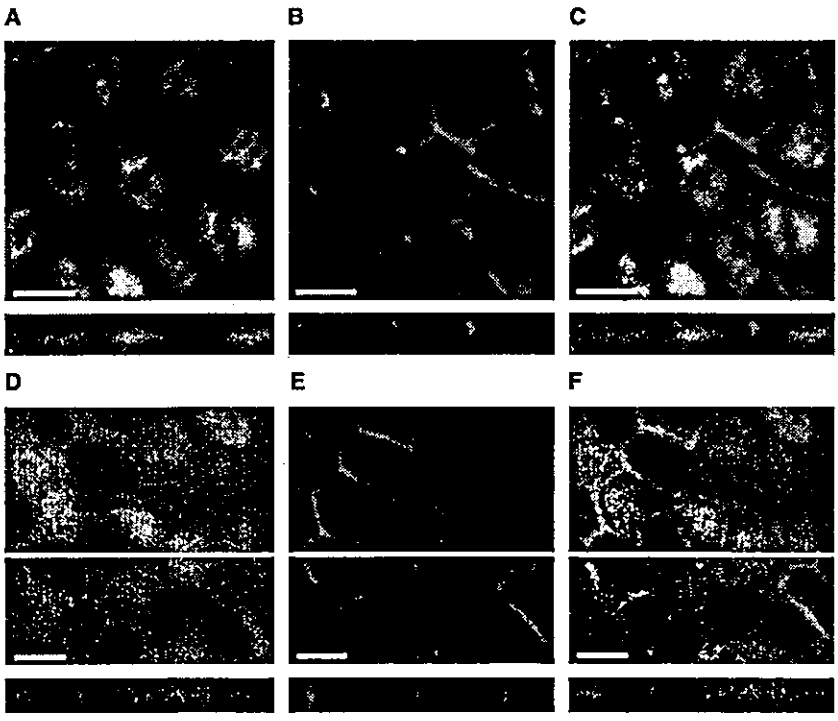

Fig. 6. Localization of Lamp1 in Madin-Darby canine kidney (MDCK) cells stably cotransfected with the wild-type and mutant aquaporin-2 (AQP2). Double staining of Lamp1 (*A*), ZO-1 (*B*), merged (*C*) or Lamp1 (*D*), Na-K-ATPase (*E*), or merged (*F*). XY and XZ sections are shown in the upper and lower panels, respectively. The samples were viewed at ×400 and white bars indicate 10 μm.

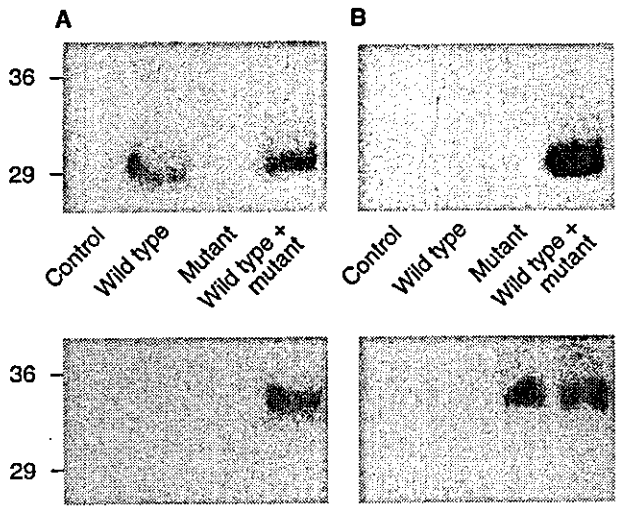

Fig. 5. Immunoprecipitation of the wild-type and mutant aquaporin-2 (AQP2) in cotransfected Madin-Darby canine kidney (MDCK) cells. (*A*) Samples were immunoprecipitated with a wild-type (WT) AQP2 antibody and immunoblotted with the same antibody (upper panel) or an antibody against mutant (M) AQP2 (lower panel). (*B*) Samples were immunoprecipitated with an antibody to the mutant AQP2 and immunoblotted with an antibody to the wild-type AQP2 (upper panel) or mutant AQP2 (lower panel).

acid proteins due to the frameshift mutation of the stop codon. Immunoblot analysis showed that the wild-type and mutant AQP2s were successfully transfected in MDCK cells (Fig. 1).

Transfected cells were grown to confluence on permeable support. The sorting of membrane channels/transporters in culture cells is generally thought to accelerate after the cells reach confluency, or more specifically, after cell polarity is rigidly established [10, 11]. Immunofluorescence microscopy suggested that the wild-type AQP2 was essentially localized at the apical membrane after forskolin treatment (Fig. 2). In contrast, the mutant AQP2 was apparently distributed at the lateral membrane (Fig. 3), with additional weak labeling of the basal membrane based on observations of the double staining with Na-K-ATPase. This difference of immunostaining in the lateral and basal membranes cannot be explained at present. However, a similar staining pattern was reported in the basolateral membrane proteins expressed in culture cells [12, 13]. In cotransfected cells, the wild-type and mutant AQP2s formed mixed oligomers that were predominantly distributed at the basolateral membrane (Figs. 4 and 5). These results suggested that the dominant-negative effect of the mutant is responsible for the mistargeting of the wild-type AQP2, leading to the pathogenesis of an autosomal-dominant–type NDI.

In cells before forskolin treatment, the wild-type AQP2 was mostly present at the apical membrane region (Fig. 2D), and apparently targeted to the apical membrane in response to forskolin (Fig. 2E). Immunoelectron microscopy of inner medullary collecting duct cells demonstrated the presence of AQP2 both in the apical plasma membrane and in small subapical vesicles, and the vasopressin-induced translocation of AQP2 to the apical membrane [14, 15]. Therefore, it might be possible that forskolin stimulated the apical trafficking of AQP2 distributed in the subapical region in our MDCK cell line. However, a detailed analysis of the protein localization was beyond the detection level of our immunocytochemistry. Immunoelectron microscopy will be necessary to prove our speculation. Contrary to cells grown on a membrane support, the wild-type AQP2 in MDCK cells grown on the coverglass was localized at perinuclear region as vesicle-like structure before forskolin treatment and homogenously localized to the apical membrane after the stimulation with forskolin [16] [unpublished observation by T. Asai). Such a characteristic distribution of AQP2 observed in cells on the coverglass might be due to the absence of rigid cell polarity. The mutant AQP2 was fundamentally present basolaterally before the incubation with forskolin (Fig. 3D). Furthermore, the red staining with antimutant AQP2 antibody was also detected just inside the lateral membrane in some cells as if a part of the mutant AQP2 were distributed there. Thus, comparison of Figure 3A and D suggested the possibility that forskolin accelerated basolateral trafficking of the mutant AQP2. However, further investigation will be required to confirm the effect of forskolin on the distribution of mutant AQP2 because our resolution of confocal microscopy is limited.

During the course of this study, Marr et al [8] reported another mutation that leads to autosomal dominant NDI in one allele of the *AQP2* gene. Interestingly, their mutant (727delG) and our mutant (763 to 772del) share an identical sequence of 66 amino acids at the C terminus. In the *Xenopus* oocyte expression system, they found that the wild-type and 727delG AQP2s formed hetero-oligomers and they were mostly retained within the cell [8]. They also reported that these hetero-oligomers were mainly localized at late endosomes/lysosomes when cotransfected in MDCK cells [8]. Our findings suggested that mixed oligomers of the wild-type and 763-772del AQP2s were basically distributed at the basolateral membrane region (Fig. 4), and apparently not predominantly localized in the late endosome/lysosome (Fig. 6), although the anti-Lamp1 antibody we used could not give a higher resolution. We cannot yet explain the reason for this discrepancy. Different sites of the mutations might explain the discrepancy. In a preliminary study, Kamsteeg et al reported another mutation (one-base insertion at C-terminus) in a patient with autosomal-dominant NDI [abstract; Kamsteeg et al, *J Am Soc Nephrol* 12:304A, 2001]. This mutation led to a replacement of the 12 C-terminal amino acids of the wild-type

AQP2 with a new C-terminal tail of 26 amino acids (QLAAEPATGYQGLRAASGLYGPDGRF). In expression studies in MDCK cells, Kamsteeg's group found basolateral localization of the mutant AQP2 and suggested that some of the amino acids at the new C-terminal were responsible for the mistargeting.

The E258K in the *AQP2* gene is the first mutation reported for autosomal-dominant NDI [5]. In contrast to the 763 to 772del mutation, the E258K mutation resulted in a retention of the mixed tetramers in the Golgi compartment in the *Xenopus* oocyte expression system [5, 6]. In most forms of autosomal-recessive NDI due to *AQP2* gene mutations, mutant proteins were misfolded and retained in endoplasmic reticulum as a monomer and not further transported to Golgi apparatus [17, 18]. A similar endoplasmic reticulum retention of misfolded proteins had been demonstrated in a number of X-linked recessive NDI cases due to *AVPR2* gene mutations [2, 3]. In addition to NDI, protein trafficking defects are also known to be responsible for a large member of congenital diseases. For example, the deltaF508 mutation found in the *CFTR* gene of cystic fibrosis patients causes protein degradation in the endoplasmic reticulum [19]. Moyer et al [20] presented evidence that the last three amino acids at the C-terminus (T-R-L) of the cystic fibrosis transmembrane conductance regulator (CFTR) comprise a PDZ-interacting domain that binds to ezrin-radixin-moesin-binding phosphoprotein 50 (EBP50), a protein that contains the PDZ domain [20]. This interaction seemed to be requisite for the apical membrane polarization of CFTR, as the S1455X CFTR mutant lacking the 26 C-terminal amino acids was mistargeted to the basolateral membrane and thereby led to the pathogenesis of cystic fibrosis [20]. In Charcot-Marie-Tooth disease, mutations of peripheral myelin protein 22 or connexin 32 lead to accumulation of the mutant protein in the endoplasmic reticulum/Golgi compartment [21, 22]. Several types of defects are known in familial hypercholesterolaemia; namely, failure to exit the endoplasmic reticulum in class 2, failure to cluster in coated pits in class 4, and failure to recycle after endocytosis in class 5 [23]. Thus, we can speculate that heterogeneous mechanisms are involved in the defects of intracellular protein trafficking.

Our results suggested that mixed oligomers of the wild-type and mutant AQP2s are mistargeted to the basolateral membrane, as well as the mutant AQP2 itself (Figs. 3 and 4). A similar molecular pathogenesis of hereditary diseases was shown only in cystic fibrosis due to the S1455X CFTR mutant, as described above. We propose two possible explanations for the mistrafficking in our case. The mutation causes either a loss of the apical targeting determinant, or an addition of a basolateral targeting determinant that dominates the intrinsic apical targeting determinant. Several determinants have been found for apical targeting. In the case of protein anchored to the cell membrane via glycerol-phosphatidylinositol (GPI), the glycolipid moiety is thought to act as an apical sorting signal [24]. However, AQP2 is not known as a GPI-anchored protein. A cluster of membrane proteins is known to move from the trans-Golgi network (TGN) to the apical surface with rafts composed of a detergent-insoluble glycolipid (DIG)-enriched complex [25]. A certain transmembrane domain is thought to interact with rafts [25]. In addition, protein traffic is generally mediated by the soluble N-ethylmaleimide-sensitive factor attachment protein (SNARE) machinery [26, 27]. Numerous SNARE-related proteins are shown to be involved in protein sorting. In the case of AQP2, vesicle-associated membrane protein 2 (VAMP2) [28], and syntaxin-4 [29] were reported to colocalize with AQP2 in the collecting duct cells. For basolateral targeting determinants in TGN, tyrosine-related and dileucine-related motifs were identified as signals to regulate localization of clathrin-coated vesicles [24]. Indeed, the sorting of AQP4 to the basolateral surface has been shown to depend on these two motifs [30]. The elongated C-terminal of our mutant AQP2 contains one dileucine motif but no tyrosine residues. Thus, the underlying mechanism of mistargeting observed in the mutant AQP2 remains unknown, and the several possibilities proposed above remain untested. Further investigations will seek to clarify the cause for this mistargeting in our NDI case.

ACKNOWLEDGMENTS

We thank Dr. E. Kominami for providing us an antibody against Lamp1. This work was supported by a Grant-in-Aid for Scientific Research and Grant-in-Aid for Scientific Research on Priority Areas from Japan Society for the Promotion of Science (JSPS).

Reprint requests to Michio Kuwahara, M.D., Department of Homeostasis Medicine and Nephrology, Graduate School, Tokyo Medical and Dental University, Tokyo 113-8519, Japan.
E-mail: mkuwahara.kid@tmd.ac.jp

REFERENCES

1. Fushimi K, Uchida S, Hara Y, *et al*: Cloning and expression of apical membrane water channel of rat kidney collecting tubule. *Nature* 361:549–552, 1993
2. Morello J-P, Bichet DG: Nephrogenic diabetes insipidus. *Annu Rev Physiol* 63:607–630, 2001
3. Nielsen S, Frokiaer J, Marples D, *et al*: Aquaporins in the kidney. *Physiol Rev* 82:205–244, 2002
4. Deen PMT, Verdijk MAJ, Knoers NVAM, *et al*: Requirement of human renal water channel aquaporin-2 for vasopressin-dependent concentration of urine. *Science* 264:92–95, 1994
5. Mulders SM, Bichet DG, Rijss JPL, *et al*: An aquaporin-2 water channel mutant which causes autosomal dominant nephrogenic diabetes insipidus is retained in the Golgi complex. *J Clin Invest* 102:57–66, 1998
6. Kamsteeg E-J, Wormhoudt TAM, Rijss JPL, *et al*: An impaired routing of wild-type aquaporin-2 after tetramerization with an aquaporin-2 mutant explains dominant nephrogenic diabetes insipidus. *EMBO J* 18:2394–2400, 1999
7. Kuwahara M, Iwai K, Ooeda T, *et al*: Three families with autosomal dominant nephrogenic diabetes insipidus caused by aquaporin-2 mutations in the C-terminus. *Am J Hum Genet* 69:738–748, 2001

8. Marr N, Bichet DG, Lonergan M, *et al*: Heteroligomerization of an aquaporin-2 mutant with wild-type aquaporin-2 and their misrouting to late endosomes/lysozomes explains dominant nephrogenic diabetes insipidus. *Hum Mol Genet* 11:779–789, 2002
9. Lefebvre B, Formstecher P, Lefebvre P: Improvement of the gene splicing overlap (SOE) method. *Biotechniques* 19:186–188, 1995
10. Handler JS: Use of cultured epithelia to study transport and its regulation. *J Exp Biol* 106:55–69, 1983
11. Horster MF, Stopp M: Transport and metabolic functions in cultured renal tubule cells. *Kidney Int* 29:46–53, 1986
12. Keller P, Toomre D, Diaz E, *et al*: Multicolor imaging of post-Golgi sorting and trafficking in live cells. *Nat Cell Biol* 3:140–149, 2001
13. Dillon C, Creer A, Kerr K, *et al*: Basolateral targeting of ERBB2 is dependent on a novel bipartite juxtamembrane sorting signal but independent of the C-terminal ERBIN-binding domain. *Mol Cell Biol* 22:6553–6563, 2002
14. Nielsen S, DiGiovanni SR, Christensen EI, *et al*: Cellular and subcellular immunolocalization of vasopressin-regulated water channel in rat kidney. *Proc Natl Acad Sci USA* 90:11663–11667, 1993
15. Nielsen S, Chou C-L, Marples D, *et al*: Vasopressin increases water permeability of kidney collecting duct by inducing translocation of aquaporin-CD water channels to plasma membrane. *Proc Natl Acad Sci USA* 92:1013–1017, 1995
16. Deen PMT, Russ JPL, Mulders SM, *et al*: Aquaporin-2 transfection of Madin-Darby canine kidney cells reconstitutes vasopressin-regulated transcellular osmotic water transport. *J Am Soc Nephrol* 8:1493–1501, 1997
17. Mulders SM, Knoers NV, Van Lieburg AF, *et al*: New mutations in the AQP2 gene in nephrogenic diabetes insipidus resulting in functional but misrouted water channels. *J Am Soc Nephrol* 8:242–248, 1997
18. Marr N, Bichet DG, Hoefs S, *et al*: Cell-biologic and functional analysis of five new aquaporin-2 missense mutations that cause recessive nephrogenic diabetes insipidus. *J Am Soc Nephrol* 13: 2267–2277, 2002
19. Cheng SH, Gregory RJ, Marshall J, *et al*: Defective intracellular transport and processing of CFTR is the molecular basis of most cystic fibrosis. *Cell* 63:827–834, 1990
20. Moyer BD, Denton J, Karlson KH, *et al*: A PDZ-interacting domain in CFTR is an apical membrane polarization signal. *J Clin Invest* 104:1353–1361, 1999
21. Sanders CR, Ismail-Beigi F, McEnery MW: Mutations of peripheral myelin protein 22 result in defective trafficking through mechanisms which may be common to diseases involving tetraspan membrane proteins. *Biochemistry* 40:9453–9459, 2001
22. Abrams CK, Oh S, Ri Y, *et al*: Mutations in connexin 32: The molecular and biophysical bases for the X-linked form of Charcot-Marie-Tooth disease. *Brain Res Brain Res Rev* 32:203–214, 2000
23. Hobbs HH, Russell DW, Brown MS, *et al*: The LDL receptor locus in familial hypercholesterolemia: Mutational analysis of a membrane protein. *Annu Rev Genet* 24:133–170, 1990
24. Matter K, Mellman I: Mechanisms of cell polarity: sorting and transport in epithelial cells. *Curr Opin Cell Biol* 6:545–554, 1994
25. Harder T, Simons K: Caveolae, DIGs, and the dynamics of sphingolipid-cholesterol microdomains. *Curr Opin Cell Biol* 9:534–542, 1997
26. Rothman JE, Warren G: Implications of the SNARE hypothesis for intracellular membrane topology and dynamics. *Curr Biol* 4:220–233, 1994
27. Hay JC, Scheller RH: SNAREs and NSF in targeted membrane fusion. *Curr Opin Cell Biol* 9:505–512, 1997
28. Nielsen S, Marples D, Mohtashami M, *et al*: Expression of VAMP2-like protein in kidney collecting duct intracellular vesicles: Co-localization with aquaporin-2 water channels. *J Clin Invest* 96:1834–1844, 1995
29. Mandon B, Chou C-L, Nielsen S, *et al*: Syntaxin-4 is localized to the apical plasma membrane of rat renal collecting duct cells: possible role in aquaporin-2 trafficking. *J Clin Invest* 98:906–913, 1996
30. Madrid R, Le Maout S, Barrault M-B, *et al*: Polarized trafficking and surface expression of the AQP4 water channel are coordinated by serial and regulated interactions with different clathrin-adaptor complexes. *EMBO J* 20:7008–7021, 2001

Kidney International, Vol. 64 (2003), pp. 102–109

Gene delivery using human cord blood–derived CD34$^+$cells into inflamed glomeruli in NOD/SCID mice

TAKASHI YOKOO, TOYA OHASHI, YASUNORI UTSUNOMIYA, AIKOU OKAMOTO, TAKAHIDE SUZUKI, JIN SONG SHEN, TADAO TANAKA, TETSUYA KAWAMURA, and TATSUO HOSOYA

Division of Nephrology and Hypertension, Department of Internal Medicine; Department of Gene Therapy, Institute of DNA Medicine; and Department of Obstetrics and Gynecology, Jikei University School of Medicine, Tokyo, Japan

Gene delivery using human cord blood–derived CD34$^+$cells into inflamed glomeruli in NOD/SCID mice.

Background. Bone marrow reconstitution using genetically-modified hematopoietic stem cells has been reported to confer resistance to inflammation and prevent renal injury in glomerulonephritis. Although this strategy has potentials for clinical use, taking hematopoietic stem cells from bone marrow is highly stressful for patients. In this regard, umbilical cord blood may be a useful alternative and, therefore, we focused on their suitability as a source of hematopoietic stem cells for transplantation-based therapy for glomerulonephritis.

Methods. CD34$^+$ cells were obtained from human umbilical cord blood, retrovirally transduced with human β-glucuronidase (HBG) gene, and transplanted into nonobese diabetic/severe combined immunodeficiency (NOD/SCID) mice. After confirming the successful chimerism, these mice were treated with lipopolysaccharide (LPS), and local HBG expression in glomeruli was examined using immunohistochemical analysis, HBG bioassay, and Western blot analysis.

Results. Clonogenic assay showed that 88.4 ± 5.9% burst-forming unit-erythroid (BFU-E), 79.7 ± 11.4% in colony-forming unit-macrophage (CFU-M), and 81.1 ± 14.1% in colony-forming unit-granulocyte (CFU-G), respectively, possessed the transgene after transfection, suggesting that precommited cells were susceptible to retroviral infection. Flow cytometric analysis revealed that 24.1 ± 14.5% of bone marrow cells in these chimera mice expressed human lymphocyte antigen (HLA) 8 weeks after transplantation. Also, clonogenic assay showed that a sustained engraftment of human hematopoietic cells expressed HBG. CD14-positive cells were recruited into the glomeruli upon LPS treatment and they secreted bioactive HBG, suggesting that cord blood–derived CD34$^+$cells may differentiate into monocyte lineage while maintaining the expression of the transgene.

Conclusion. These data indicate that umbilical cord blood cells can be utilized as a source of hematopoietic stem cells for the transplantation-based therapy of glomerulonephritis.

Recently, stem cell research has attracted considerable attention from many researchers because it could be used for organ regeneration after untreatable damage, and several stem cells (or progenitor cells), such as endothelial stem cells [1] and neural stem cells [2] have been discovered. Following the progression of this field of research, the potential for stem cell therapy has increased and several therapeutic benefits have already been reported [3, 4]. Although this approach was originally investigated for fatal or hereditary diseases, we have proposed that inflammatory diseases such as glomerulonephritis are also candidates for transplantation-based gene therapy using hematopoietic stem cells [5]. We used bone marrow–derived cells as a vehicle to deliver anti-inflammatory molecules into inflamed glomeruli [6, 7]. In the ex vivo differentiation system, bone marrow cells were differentiated ex vivo to express ligands of adhesion molecules and acquire the potential to be recruited to the inflamed site, and were adenovirally transfected with a foreign gene followed by transfusion to the affected subjects. These cells may deliver anti-inflammatory cytokines into inflamed glomeruli [8]. In the in vivo differentiation system, bone marrow cells were genetically modified using retrovirus and transplanted to the affected subjects before differentiation so that they may retain the potential for self-renewal, as well as differentiation, in vivo [7]. Both systems were able to prove the therapeutic benefit of anti-glomerular basement membrane (anti-GBM) nephritis in mice [6, 7]. These strategies have several advantages over the previous glomerulus-targeted gene delivery systems (i.e., use of peripheral vessels for administration, longer therapeutic time window, and possibly no immunoreaction due to autologous transfer) and suggest that bone marrow–derived cells can be utilized for therapeutic intervention to treat local inflammation.

As a next step toward clinical application, we sought a different source of hematopoietic stem cells other than bone marrow, since taking stem cells from bone marrow is highly inconvenient for patients, especially when it is for the treatment of nonlethal diseases like inflammation.

Key words: stem cell, CD34, NOD/SCID mouse, gene delivery, glomerulonephritis.

Received for publication March 25, 2002
And in revised form November 27, 2002
Accepted for publication February 14, 2003

In this regard, umbilical cord blood cells may be a useful alternative because: *(1)* a substantial amount of blood (about 100 mL from each delivery [9]) may be corrected without pain and risk to mother or infant; *(2)* they contain a significantly higher number of hematopoietic progenitor cells when compared with adult peripheral blood [10]; *(3)* lower incidence and severity of graft versus host disease (GVHD) after transplantation occurs due to the immature immune system [10]; and *(4)* recently, large-scale banks of cord blood have been developed or are being considered throughout world. We, therefore, examined their suitability as a source of hematopoietic stem cells for transplantation-based gene therapy for inflammatory diseases.

To monitor the behavior of human cells in vivo, a bone marrow repopulating system using the nonobese diabetic/severe combined immunodeficiency (NOD/SCID) mouse was applied. NOD/SCID mice are characterized by a functional deficit of natural killer cells, absence of circulating complement, and defects in the differentiation and function of antigen-presenting cells (APC), as well as an absence of T and B cell functions, facilitating reconstitution with human hematopoietic cells [11, 12]. Using transplantation techniques, chimera mice, which have a mouse body with a human hematopoietic system, may be established.

In this study, we report that umbilical cord blood cells may be a useful alternative as a source of hematopoietic stem cells for transplantation-based gene therapy to treat inflammatory diseases such as glomerulonephritis.

METHODS

Experimental Design

$CD34^+$ cells were obtained from human cord blood and retrovirally transfected with human β-glucuronidase (HBG) as a marker. Successful transfection into predifferentiated cells was confirmed by clonogenic assay. These cells were transplanted into NOD/SCID mice, and 8 weeks later successful chimerism was again confirmed by clonogenic assay and flow cytometric analysis. Since we found that LPS induced adhesion molecules even in the glomeruli of NOD/SCID mice (data not shown), these chimera mice received 25 μg LPS purified from *Klebsiella* O3 [13] or saline as a control for 7 days. Tissue specimens were subjected to immunohistochemical analysis on human CD14 and HBG to confirm that the transplanted premature cells may differentiate into monocyte lineage cells at the recruited site and those cells still express transgene. HBG bioactivity and Western blot analysis of isolated glomeruli were also compared between LPS-treated and saline-treated mice.

Animals

A breeding colony of NOD/SCID mice was established at the laboratory animal center of the Jikei University School of Medicine (Tokyo, Japan) from breeding pairs purchased from Jackson Laboratory (Bar Harbor, ME, USA). Animals were housed in a positive airflow ventilated rack and bred and maintained under specific pathogen-free conditions.

Establishment of chimera mice

Human umbilical cord blood samples were obtained, with informed consent, from placentas of full-term normal newborn infants. After isolation of mononuclear cells from cord blood by density gradient centrifugation with Nicoprep™ 1.077 (Nycomed Pharma AS, Oslo, Norway), $CD34^+$ cells were obtained from mononuclear cells by magnetic bead separation (Dynal CD34 Progenitor Cell Selection System; Dynal, Lake Success, NY, USA) according to the manufacturer's instructions. These cells were suspended in MyeloCult H5100 (StemCell Technologies, Inc., Vancouver, British Columbia, Canada) with penicillin G (100 U/mL), streptomycin (100 μg/mL), and amphotericin B (0.25 μg/mL) supplemented with 200 units/mL human interleukin-6 (IL-6) (Kirin Brewery Co., Ltd., Tokyo, Japan), and 100 ng/mL human stem cell factor (mSCF) (Kirin Brewery Co., Ltd.), Flt-3/Flk-2 ligand (100 ng/mL; R & D Systems, Minneapolis, MN, USA), human thrombopoietin (10 ng/mL; Kirin Brewery Co., Ltd.). After cultivation in a humidified atmosphere of 5% CO_2 at a concentration of 1×10^6 cells/mL for 24 hours, the bone marrow cells were transfected with the human HBG gene via a retrovirus as described later. NOD/SCID mice were prepared for transplantation with a sublethal dose of irradiation (3.5 Gy). Genetically-modified $CD34^+$ cells (5×10^4/20 g body weight) were infused into recipient mice via the tail vein once daily for 4 consecutive days. Bone marrow cells were freshly prepared for each injection.

Recombinant retrovirus preparation and infection

$CD34^+$ cells were transduced with HBG via a retrovirus using a centrifuge method [14]. ψCRIP packaging cells [15] producing an MFG-GC vector (1×10^6 cfu/mL) expression of HBG were constructed as described before [16]. A retroviral vector–containing supernatant was collected from confluent monolayers of these packaging cells grown in Dulbecco's modified Eagle's medium (DMEM) with 10% calf serum (CS) (Gibco/BRL, Grand Island, NY, USA). These supernatants were filtered (0.45 μm) and centrifuged at 14,000 g for 2 hours at 4°C to concentrate the virus [17], followed by resuspension in one-tenth the volume of culture medium. After pre-stimulation with IL-6, hSCF, thrombopoietin, and Flt-3/Flk-2 ligand for 24 hours, $CD34^+$ cells (5.0×10^4/mL culture medium) were transferred into a round-bottomed tube (Falcon #2051, Franklin Lakes, NJ, USA), which was coated with a recombinant human fibronectin fragment CH-296 (Takara Shuzo Co., Ltd., Shiga, Japan)

[18], mixed with the same amount of concentrated retroviral vector and 8 μg/mL polybrene and centrifuged at 1500 g at 20°C for 2 hours once daily for 3 days [14]. Freshly prepared retroviral vector–containing supernatant was used for each period of infection. Between centrifugations, the cells were incubated with culture medium in the presence of IL-6, hSCF, thrombopoietin, and Flt-3/Flk-2 ligand without transfer from the centrifuge tube. After the third centrifugation, $CD34^+$ cells were washed and resuspended in phosphate-buffered saline (PBS) for transplantation.

Fluorescence cytometry

Bone marrow cells were harvested from chimera mice 8 weeks after transplantation and incubated with mouse immunoglobulin G (IgG) and fluorescein isothiocyanate (FITC)-conjugated anti-human HLA ABC antigen (Sigma, St. Louis, MO, USA) for 30 minutes and 60 minutes, respectively, at 4°C. Samples were analyzed on a flow cytometer (Becton Dickinson, Franklin Lakes, NJ, USA). Four chimera mice were analyzed individually. As a positive control, mononuclear cells from healthy volunteers were also subjected to flow cytometric analysis.

Clonogenic assay for transduced $CD34^+$ cells

Clonogenic assay was performed as previously described [19]. In brief, transduced $CD34^+$ cells were plated at a concentration of 1×10^3 cells/mL in MethoCult GF H4434V (methylcellulose-containing medium with erythropoietin, stem cell factor, GM-CSF, and IL-3) (StemCell Technologies, Inc.). After 14 days, CFU-G, CFU-M, and BFU-E were selected and DNA was extracted following a previously published method [20]. The yield of DNA was monitored by human-specific β_2 microgloblin polymerase chain reaction (PCR) [21]. To amplify the HBG cDNA sequence, PCR was carried out on genomic DNA samples in a final volume of 100 μL. The primers used for PCR were 5′-GAT GGT GAT CGC TCA CAC CA-3′ and 5′-CGG TGA CTG TTC AGT CAT GA-3′, which amplify part of the HBG cDNA sequence. The reaction mixture contained 250 μmol/L of each desoxynucleoside triphosphate (dNTP), 2.5 units of Amplitaq Gold (Perkin Elmer, Foster City, CA, USA), 2.5 mmol/L $MgCl_2$, and 0.5 μmol/L of each primer in Amplitaq buffer. Thermal cycling was performed on Takara PCR Thermal cycler MP (Takara Shuzo Co., Ltd.) as follows: 95°C for 5 minutes for initial denaturing, followed by 63 cycles of 94°C for 1 minute, 60°C for 1 minute, and 60°C for 5 minutes for the final extension cycle. After electrophoresis in a 2% agarose gel, the amplified products were visualized with ethidium bromide staining. Experiments were performed in quadruplicate and representative pictures are shown.

Two-color immunofluorescent staining

Each specimen was embedded in optimal cutting temperature (OCT) compound (Miles Scientific, Naperville, IL, USA) and quickly frozen in liquid nitrogen. Cryostat sections (6 μm) were dried and fixed with acetone for 15 minutes. After blocking the endogenous biotin with an avidin/biotin blocking kit (Vector Laboratories, Burlingame, CA, USA), the sections were incubated with sheep anti-human CD14 (Genzyme, Cambridge, MA, USA) and goat anti-human HBG (a kind gift from Dr. William S. Sly) at 4°C overnight and biotinylated donkey anti-sheep IgG (Chemicon, Temecula, CA, USA) for 2 hours at 37°C. After rinsing in PBS, the sections were incubated with Alexa Fluor® rabbit anti-goat IgG (H+L) conjugate (Molecular Probes, Leiden, The Netherlands) and FITC-streptavidin (Becton Dickinson, Franklin Lakes, NJ, USA). The sections were mounted in p-phenylenediamine (PD)-PBS-glycine and observed under a fluorescence photomicroscope. Pictures were taken using an autoexposure camera (Zeiss, Thornwood, NY, USA).

HBG enzymatic activity of isolated glomeruli

HBG bioactivity of isolated glomeruli was assayed as described [22]. Briefly, glomeruli from chimera mice transplanted with LPS or saline treatment were isolated and homogenized in distilled water using a glass homogenizer. The homogenates were spun at 14,000*g* for 10 minutes at 4°C. The clear supernatant was assayed fluorometrically for HBG activity with the synthetic fluorogenic substrate 4-methylumbelliferyl β-D-glucuronidase (Sigma). After incubation of each sample with the substrate for 30 minutes at 37°C, reactions were terminated by the addition of 0.17mol/L glycine-carbonate buffer (pH 10.4). The 4-methylumbelliferone (4-MU) that had formed was measured fluorometrically. Units of HBG activity are defined as nanomoles 4-MU produced/hr/mg protein. Protein concentration was determined with a bicinchorinic acid (BCA) kit (Pierce, Rockford, IL, USA).

Immunoprecipitation of human HBG

Since measurements of HBG enzymatic activity were made both of total HBG activity representing the endogenous murine HBG activity and any human HBG activity resulting from gene transfer, immunoprecipitation of human HBG was performed to estimate the human HBG activity only. Each sample was divided into two identical aliquots and the human HBG was immunoprecipitated from one of each pair. Ten micrograms of protein of each homogenate were mixed with either 10 μL of anti-human HBG or distilled water, and shaken at 4°C for 1 hour. Twenty five microliters of protein A sepharose 4 fast flow® (Amersham Pharmacia Biotech, Buckinghamshire, UK) was then added to each of the samples, which were inverted overnight at 4°C. Samples were spun at